2007

Deformation of the Douglas till, northwestern Wisconsin

Jacqueline Rose Shumway
Iowa State University

Deformation of the Douglas till, northwestern Wisconsin

by

Jacqueline Rose Shumway

A thesis submitted to the graduate faculty

in partial fulfillment of the requirements for the degree of

MASTER OF SCIENCE

Major: Geology

Program of Study Committee:
Neal R. Iverson, Major Professor
Carl Jacobson
Jonathan Sandor

Iowa State University

Ames, Iowa

2007

UMI Number: 1451091

ProQuest Information and Learning Company
300 North Zeeb Road
P.O. Box 1346
Ann Arbor, MI 48106-1346

TABLE OF CONTENTS

ACKNOWLEDGEMENTS

I would like to acknowledge the many people that helped me throughout my research. First and foremost I would like to thank my advisor, Neal Iverson, for giving me the opportunity to come work with him and providing a great deal of guidance during each stage of my graduate studies at Iowa State University. I would also like to acknowledge my other Program of Study committee members: Carl Jacobson and Jonathan Sandor. Pete Moore also deserves special thanks for helping me during my first few trips to northwestern Wisconsin, as well as for having many lengthy discussions with me about my research. I would like to thank Obe and Mark Saarie for giving me access to my field site at Bardon Creek and for their generosity during my stays in Douglas County. Heather Bleick and Al and Maria Marciulionis helped collect numerous field samples for which owe I them a great deal of thanks. I would also like to acknowledge Mike Jackson, Basil Tikoff, and JoAnn Gage for letting me use their Kappabridges for the many long hours it took to analyze samples. Finally, I would like to thank my family, especially my fiancé Adam, for their continuous encouragement and support. Without them I would not have come as far as I have today.

ABSTRACT

The bed-deformation model asserts that a glacier can move by pervasively shearing its bed to strains sufficiently large to account for most glacier motion (>100). Although commonly invoked, this hypothesis has never been unequivocally tested using the geologic record. In this study, laboratory fabric-strain calibrations are used to evaluate strain magnitude and shear direction in the Douglas till of northwestern Wisconsin and to thereby test elements of the bed-deformation hypothesis. The Douglas till is a clay-rich basal till deposited by a late-Wisconsinan advance of the Superior lobe of the Laurentide ice sheet. This till contains unusual pebble fabrics that lie transverse (NW-SE) to the regional ice-flow direction (NE-SW), as indicated by flutes.

Anisotropy of magnetic susceptibility (AMS) was measured along eight vertical profiles through the Douglas till at 0.2 m intervals, and AMS fabrics were computed from principal directions of magnetic susceptibility. Sand-particle fabrics and microshear orientations were also measured in one of these profiles. AMS data were interpreted using results of ring-shear experiments, which demonstrated that strong, flow-parallel fabrics (steady-state S_1 eigenvalue of 0.83) develop in the Douglas till at a shear strain of ~20.

AMS fabrics are generally strong (63% of $S_1 \geq 0.83$), indicating that most of the till has been sheared to a strain ≥ ~20. Sand-particle and AMS fabrics were similarly oriented, and microshears indicate fabric development was subglacial, rather than in shearing basal ice. Major variations in fabric orientation and strength occur laterally over distances of a few meters and with depth over decimeters, indicating that the till

deformed heterogeneously, probably during progressive accretion of till to the bed by lodgement. Strong fabrics transverse to the regional glacier-flow direction are interpreted to reflect shear divergence or convergence in a heterogeneously deforming bed, resulting in local flow directions commonly perpendicular the regional one. These measurements indicate that deep, unidirectional, simple shear of the bed, as is usually assumed in models, was unlikely.

CHAPTER 1. BACKGROUND AND OBJECTIVES

A. Bed-deformation model

One commonly invoked glacier-flow mechanism is pervasive bed deformation (e.g., Alley et al., 1986; 1987; Boulton and Hindmarsh, 1987; Clark, 1997). The bed-deformation model of glacier flow asserts that a glacier moves primarily by shearing its bed, usually assumed to consist of till, such that the till undergoes very high shear strains (Figure 1.1). This is an important process because past ice sheets resting on thawed, unlithified sediment may have moved by deforming their beds (Alley, 1991; Boulton, 1996; Clark, 1997), which would have affected their dynamic response to climate variability (Clark et al., 1999). Bed deformation may have also played an important role in sediment transport (Alley, 1991) and glacial landform development (e.g., Boulton, 1987; Clark, 1991; Clark and Walder, 1994; Johnson and Hansel, 1999) during past glaciations and may provide an explanation for the fast flow of some modern glaciers and ice streams (Alley et al., 1986; Truffer et al., 2000).

Although bed deformation has been widely invoked as a glacier-flow mechanism, its influence on glacier flow is still unknown and has never been unequivocally tested using the geologic record. Vast areas of Europe and North America are covered with basal tills that were left behind by past ice sheets. These tills may contain information about their deformational histories (e.g., Alley, 1991; Clark and Walder, 1994; Clark, 1997). As a result, numerous field studies have been conducted in attempts to further understand subglacial deformation of sediments. These studies have yielded abundant evidence suggesting glaciers deform their beds (e.g., van der Meer, 1993; Hart and

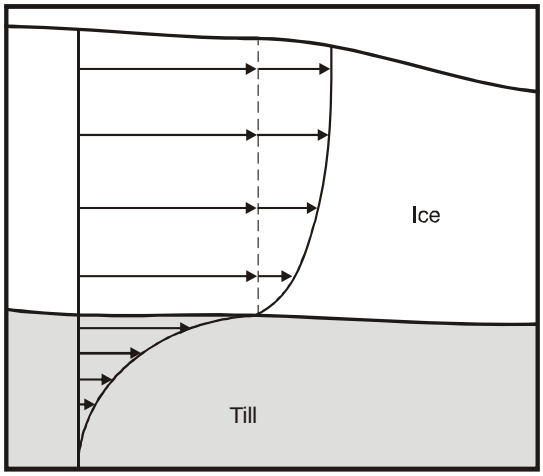

Figure 1.1. Schematic diagram showing the vertical profile through a glacier moving primarily by shearing its till bed. The thickness of the till relative to the ice is exaggerated.

Roberts, 1994; Menzies, 2000; van der Wateren, 2000; van der Meer et al., 2003; Menzies et al, 2006), but have provided virtually no information regarding the extent of this deformation. As a result, no consensus regarding diagnostic characteristics of till pervasively deformed to the high strains required of the bed-deformation model has resulted from these studies (e.g., Hart et al., 1996; Piotrowski et al., 1997; Boulton et al., 2001; Piotrowski et al., 2001; Piotrowski et al., 2002).

B. Till fabric

Fabric is a characteristic of tills that is commonly measured to help elucidate subglacial processes. Simply defined as the degree of alignment of non-equant grains in sediment, fabric can be measured at various scales. Gravel and sand-sized particle fabrics are most commonly measured in field studies (e.g., Evenson, 1971; Lawson, 1979; Johnson, 1983; Dowdeswell et al., 1985, Ham and Mickelson, 1994; Hart, 1994; Benn, 1995; Yi and Cui, 2001; Larsen and Piotrowski, 2003; Carr and Rose, 2003;

Thomason, 2006). Another technique involves measuring the anisotropy of magnetic susceptibility (Fuller, 1964; Boulton, 1971; Gravenor et al., 1973; Stupavsky et al., 1974; Gravenor and Stupavsky, 1975; Stupavsky and Gravenor, 1975; Eyles et al., 1987, Stewart et al., 1988; Principato et al., 2005) of multiple intact samples, which yields information about the alignment of non-equant magnetic particles.

Many fabric studies have attempted to use fabric strength to distinguish tills that have been pervasively deformed from those that have been deposited by other processes, such as lodgement and subglacial melt-out. Interpretations from these studies are based on the idea that different strengths of fabrics can be correlated to specific depositional processes (Dowdeswell and Sharp, 1986; Hicock, 1992; Hicock and Dreimanis, 1992; Hart, 1994; 1995; 1997; Hart et al., 1996; Hicock et al., 1996; Clark, 1997; Lian et al., 2003; Carr and Rose, 2003). However, such inferences are derived from fabric measurements in tills where unequivocal independent evidence of governing depositional processes is usually lacking. This ambiguity has resulted in contradictory interpretations of till fabric (e.g., Boulton et al., 2001; Piotrowski et al., 2001). Recent studies suggest that fabric cannot be used to distinguish between modes of till deposition (e.g., Bennett et al., 1999; Larsen and Piotrowski, 2003; Boulton et al., 2001; Iverson et al., in press). This is a reasonable conclusion because modes of till deposition are not likely correlated in a simple way to the extent of particle rotation caused by deformation of either the bed or sediment-laden basal ice.

Although till fabric cannot be used as a facies discriminator, it can be used as an indicator of strain magnitude, which is valuable for testing the bed-deformation model. Even for short periods of glacier occupation (e.g., 100 yr), thick shearing beds (e.g., 5 m),

and low basal-flow velocities (e.g., 10 m yr^{-1}), a shear strain (horizontal displacement divided by shearing-layer thickness) of greater than 100 is required for most glacier motion to occur by bed deformation. Knowing the magnitude to which till has been sheared is essential for determining whether or not glaciers moved primarily by deforming their beds. A major problem with most field studies that have attempted to use till fabric to assess the bed-deformation model is that the relationship between till fabric and shear-strain magnitude is essentially unknown.

An obvious way to determine this relationship is to conduct experiments. In experiments shear-strain magnitude can be controlled and easily measured. The lack of consensus regarding the relationship between shear-strain magnitude and fabric strength has prompted experimental work in recent years (Hooyer and Iverson, 2000; Thomason and Iverson, 2006; Hooyer et al., in press; Iverson et al., in press). In these experiments samples of till were sheared up to strains of ~714 in a ring-shear device, and fabric strength was measured at increasing increments of strain. Results indicated that grains rotate so that their long axes become parallel to the shearing direction at relatively low strains (~7-30), and remain there with increasing strain. The result is that strong, steady-state fabrics develop at moderately low strains. Grains in this steady state also plunge gently "upglacier".

These results suggest that tills that have been sheared to the high strains (>100) required by the bed-deformation model should exhibit strong, flow-parallel fabrics, contrary to the predictions of the Jeffery (1922) model for particle rotation in a slowly

shearing viscous fluid. This conclusion is important because the Jeffery (1922) model is commonly used by glacial geologists to explain either weak till fabrics or fabric modes transverse to the glacier-flow direction (Glen et al., 1957; MacClintock and Dreimanis, 1964; Hart, 1994; Hicock et al., 1996; Clark, 1997; Lian et al., 2003; Carr and Rose, 2003). The Jeffery model yields false predictions for fabric development in till due to the no-slip boundary condition that is assumed in the model at particle surfaces; in reality the till matrix slips across the surfaces of particles, which keeps them from undergoing the continuous, end-over-end particle rotation of the Jeffery model (Hooyer and Iverson, 2000; Iverson et al., in press).

C. Microshears

Microshears are another structural feature that may be used to assess the deformational history of tills. The progressive development of microshears with increasing strain has been studied in ring-shear experiments, in which till was sheared up to strains of 108 (Thomason and Iverson, 2006; Larsen et al., 2006). In these experiments two sets of microshears developed at predictable angles (Riedel shears) during the initial stages of shearing (Figure 1.2). At shear strains of $> \sim 10$, these microshears become more pervasive and parallel to the plane of shearing (Thomason and Iverson, 2006). This is similar to microshear development observed in experiments with clay (e.g., Morgenstern and Tchalenko, 1967) and fault-gouge (e.g., Logan et al., 1992). Thomason and Iverson (2006) concluded that particle-fabric orientations in sheared till reflect time-integrated rotation of particles due to movement along Riedel shears, which

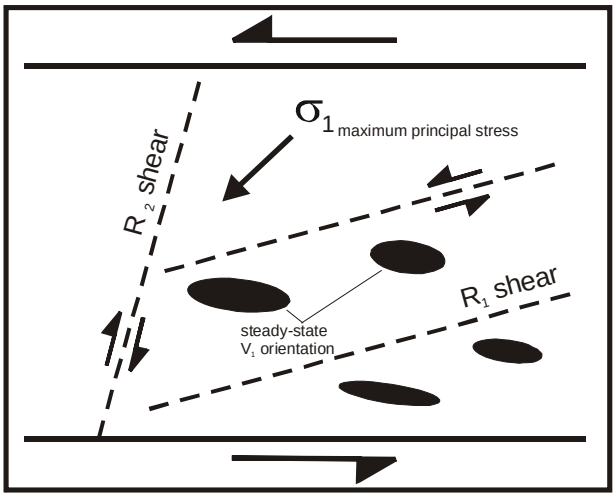

Figure 1.2. Schematic showing Riedel shear orientations that developed in till during ring-shear experiments (from Thomason and Iverson, 2006). Black ellipses show the orientations of particles.

can explain the tendency for particles to plunge up-glacier (see Larsen et al., in press, for a similar argument). Larsen et al. (2006) found that at shear strains of > ~18, microshear development reached a steady state.

The simple presence of microshears is useful in making the distinction between particle alignment that has resulted from deformation within sediment-laden basal ice and from deformation of the bed. This is because microshears are not expected to develop in ice during shear, owing to the fluid behavior of ice (Thomason and Iverson, 2006). On the other hand, microshears will develop in till that has sheared beneath the ice because till behaves as a Coulomb (frictional) plastic material (e.g., Iverson et al., 1998; Tulaczyk et al., 2000). Thus, if microshears are present in till, then deformation after sediment deposition from ice is implied. In addition, as noted previously, the plunges of microshears may help to identify till that has been sheared to high strains.

D. Testing the bed-deformation model

Given the potential effect of bed deformation on glacier dynamics, sediment transport, and landform development, the bed-deformation model needs to be tested. Perhaps the only convincing way to do so using the geologic record is by combining experiments with field studies. Experiments allow fabrics to be used to place definitive limits on shear-strain magnitude and direction in till (Iverson et al., in press). The aim of this study was to conduct a detailed microstructural field study of a basal till and use these experimental results to interpret the nature of the till's deformation. This approach allows us to move a step closer to testing the bed-deformation model.

E. Douglas till of the Superior lobe

The Douglas till of the Miller Creek formation in northwestern Wisconsin (Figure 1.3a) was chosen for this study. The Douglas till is the surficial glacial deposit in much of northern Douglas and northwestern Bayfield counties and is exposed in the upper portion of the bluffs along the shoreline of Lake Superior (Figures 1.3, 1.4). It was deposited by the Superior lobe of the Laurentide ice sheet during its last advance (Lake View advance) into Wisconsin (Figure 1.3b), about 11,000 years ago (9,600 ^{14}C years (Clayton, 1984) corrected to calendar years following Stuiver et al. (1998)), and most likely correlates with till associated with the Nickerson phase of the Superior lobe in Minnesota (Wright et al., 1973; Need and Johnson, 1980). The Douglas till is composed of approximately 11% sand, 26% silt, and 63% clay, with pebbles, cobbles, and boulders present but scarce (Need, 1980; Johnson, 1980; 1893). The till occurs as a thick (up to

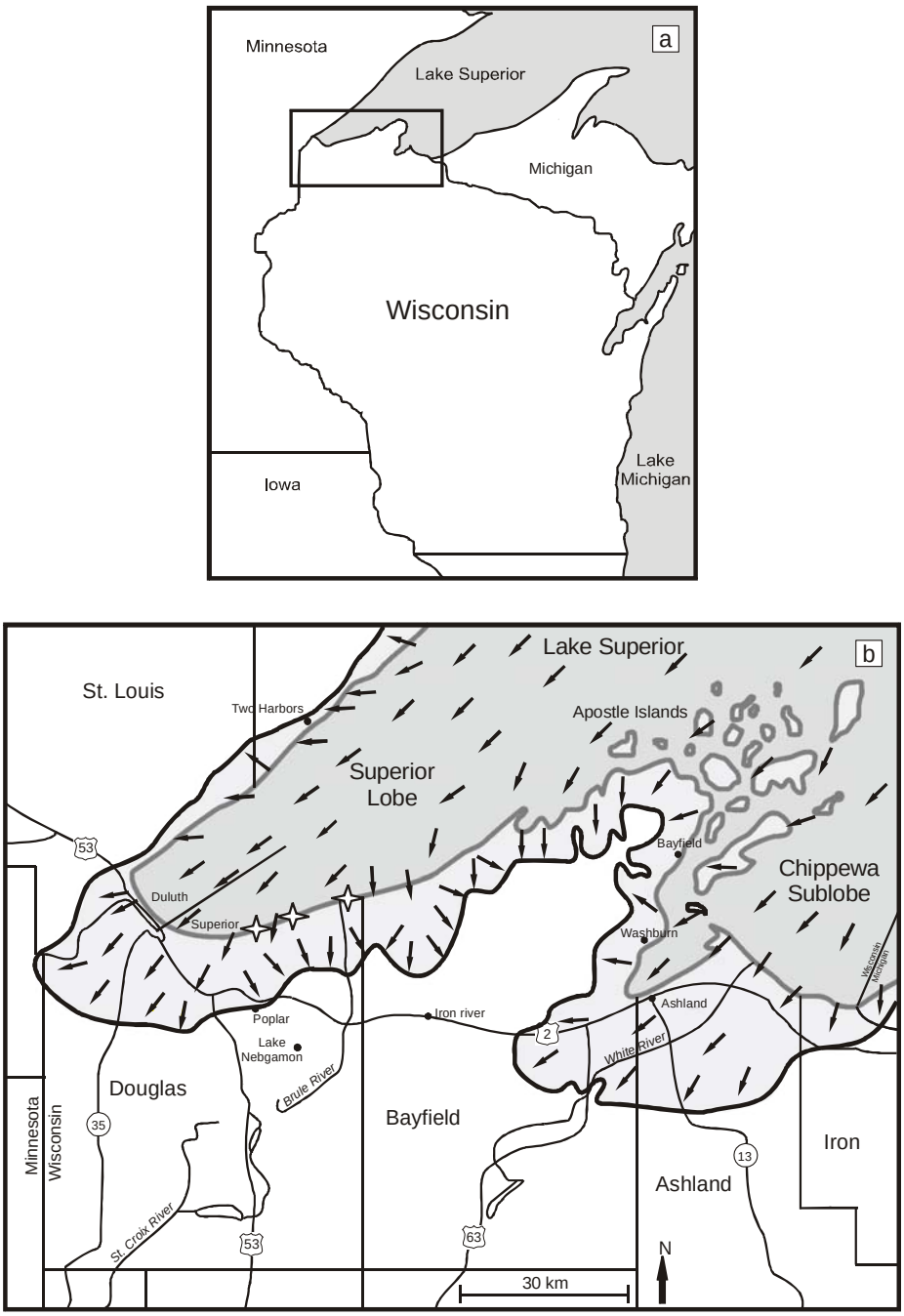

Figure 1.3. (a) Location of Douglas member in northwestern Wisconsin. (b) Position of the Superior lobe during deposition of the Douglas member (Lake View advance) (from Clayton, 1984). Stars indicate sample site locations from this study.

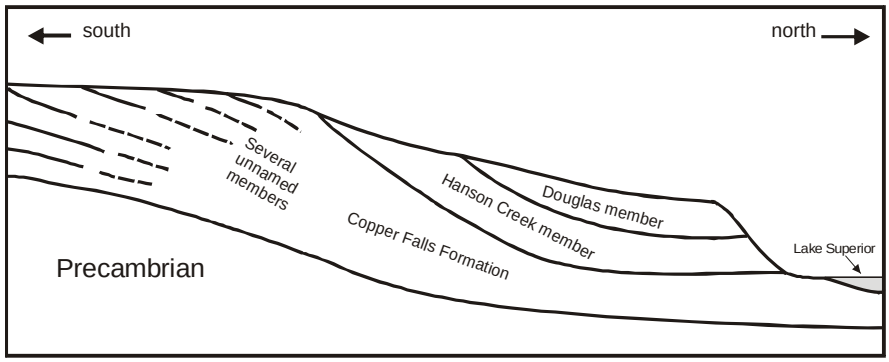

Figure 1.4. Schematic cross-section showing stratigraphy of northwestern Wisconsin (after Clayton, 1984).

15 m), massive deposit and becomes increasingly fine-grained to the west (Need, 1980). It is informally known as "red clay" for its reddish-brown color and high clay content.

Underlying the Douglas till is the Hanson Creek member of the Miller Creek formation, which is exposed in the lower portions of the bluffs along Lake Superior (Figure 1.4). It is similar in texture to the Douglas till, on average containing 11% sand, 32% silt, and 57% clay, and similarly contains few gravel-sized and larger clasts. However, the Hanson Creek member is browner in color and has gray/green and dull reddish-brown stringers of silty material, which gives it a marbled appearance (Johnson, 1980; Need, 1980).

The Copper Falls formation underlies the Miller Creek formation and is the surficial deposit of Douglas and Bayfield counties southward of where the Douglas and Hanson Creek members are exposed at the surface (Figure 1.4) (Clayton, 1984). It is typically a sandier unit than the overlying Miller Creek formation and contains several members that have not been formally recognized (Clayton, 1984). In northwestern

Wisconsin the Copper Falls formation has been informally called the Jardine Creek till unit by Need (1980). The unit contains an average of 61% sand, 24% silt, and 15% clay and is reddish-brown in color (Need, 1980). Its exposure along the shoreline of Lake Superior is discontinuous and restricted to the very bottom of the bluffs.

The "red clay" of northwestern Wisconsin has largely been of interest because of its great thickness, massive texture, and low pebble, cobble, and boulder content. Early researchers, as described by Johnson (1983), assumed it had a lacustrine origin, attributing the rare pebbles, cobbles, and boulders to ice rafting, and the clay's lack of laminations to deposition within deep-water areas containing few currents (e.g., Moss, 1977; Zarth, 1977). Although some researchers did suggest that the clay might be of subglacial origin, the evidence cited for it was weak. Because of this uncertainty, Johnson (1980; 1983) conducted a field study of the Miller Creek formation and found evidence supporting the idea that both the Douglas and Hanson Creek members were tills rather than lake sediments. This evidence included striated boulder pavements at the base of the Douglas member, low-relief flutes on the surface of the Douglas member, macro- and microfabrics in both members, and the presence of shear planes. He also used the areal extent, outcrop characteristics (massive texture), and grain-size trends to support his conclusions. Another interesting result of Johnson's (1980; 1983) study is that some of the fabrics he measured were oriented transverse to the regional ice-flow direction. He interpreted the ice-flow direction to be parallel to the flutes that he described.

The Douglas till was chosen as the focus of this study for several reasons. Late-Wisconsinan/early-Holocene advances of lobes of the Laurentide ice sheet are of interest

due to the rapidly warming climate of that period and the implication that such advances may have been triggered by internal glacier dynamics, including possibly bed deformation. A modern analog may be the well-documented speed-up of outlet glaciers of the southern two-thirds of the Greenland ice sheet during the last decade, thought by some to be a dynamic response to global warming (Rignot and Knagaratnam, 2006; Howat et al., 2005). The transverse fabrics measured by Johnson (1980; 1983) were also of interest. Transverse or weak fabrics are commonly interpreted to be the result of pervasive bed deformation. However, as noted, results from ring-shear experiments contradict that assumption, which means a new explanation for transverse fabrics needs to be developed. Another reason for choosing the Douglas till for this study was because it has high clay and low carbonate content. These characteristics were important because microshears develop better in clay-rich materials (Skempton, 1985; Morgenstern and Tchalenko, 1967) and the visibility of microshears, which are seen as birefringent lineaments in thin section, can be obscured by carbonate minerals which are also birefringent in thin section (van der Meer, 1993; Thomason and Iverson, 2006). The Douglas till has the added benefit of being easily accessible due its exposure along Lake Superior and relatively easy to sample due to its high clay and low gravel content. Finally, if Johnson's (1989; 1983) interpretation of the Douglas member as a basal till is correct, then it is likely that this unusually fine-grained till was derived from overridden lake sediments. The characteristic microfabric of lake sediments is well-known (e.g., Tarling and Hrouda, 1993), so the Douglas till offers a rare opportunity to study a till in which the fabric of the protolith can be inferred with some confidence.

F. Objectives

The goal of this research was to study microstructural characteristics of the Douglas member—primarily fabrics defined by the till's anisotropy of magnetic susceptibility (AMS)—to answer the following questions:

1) Is the Douglas member really a till?
2) Were parts or all of it deformed to the high strains required by the bed-deformation model?
3) What is the origin of the member's transverse fabrics?
4) Was the Douglas member transported in a thick, uniformly deforming bed?

CHAPTER 2. METHODS

A. Introduction

This study focuses on three types of microstructural characteristics of till: AMS fabric, sand-particle fabric, and microshear orientations. AMS fabrics were measured in multiple vertical sections of the Douglas till and sand-particle fabrics and microshear orientations were measured in one of these sections. Results of ring-shear experiments using the Douglas till provided a foundation for interpretations.

B. Sampling program

Three sample sites were chosen in northern Douglas County, Wisconsin, in areas where the Douglas till is exposed in bluffs along the shoreline of Lake Superior (Figure 2.1a). These sites are located near the mouths of the Middle River (MR), Bardon Creek (BC), and Brule River (BR), which all drain north into Lake Superior (Figure 2.1b). Samples were collected during the summer of 2006, from mid-May to mid-June and from mid-July to mid-August.

Samples were collected at each site for measuring AMS fabric, sand-particle fabric, and microshear orientations from 0.2 m depth intervals in multiple vertical profiles. Two profiles were sampled at Brule River (BR2-BR3), four profiles were sampled at Bardon Creek (BC2-BC5), and two profiles were sampled at Middle River (MR3-MR4) (Figure 2.2). The elevation spanned by each profile varied from site to site. At Brule River both profiles ranged from 3.2 m to 5.0 m above lake level and were limited in extent by the modest height of the exposure. At Bardon Creek the total range sampled was from 9.0 m to 16.8 m above lake level. However, the ranges differed

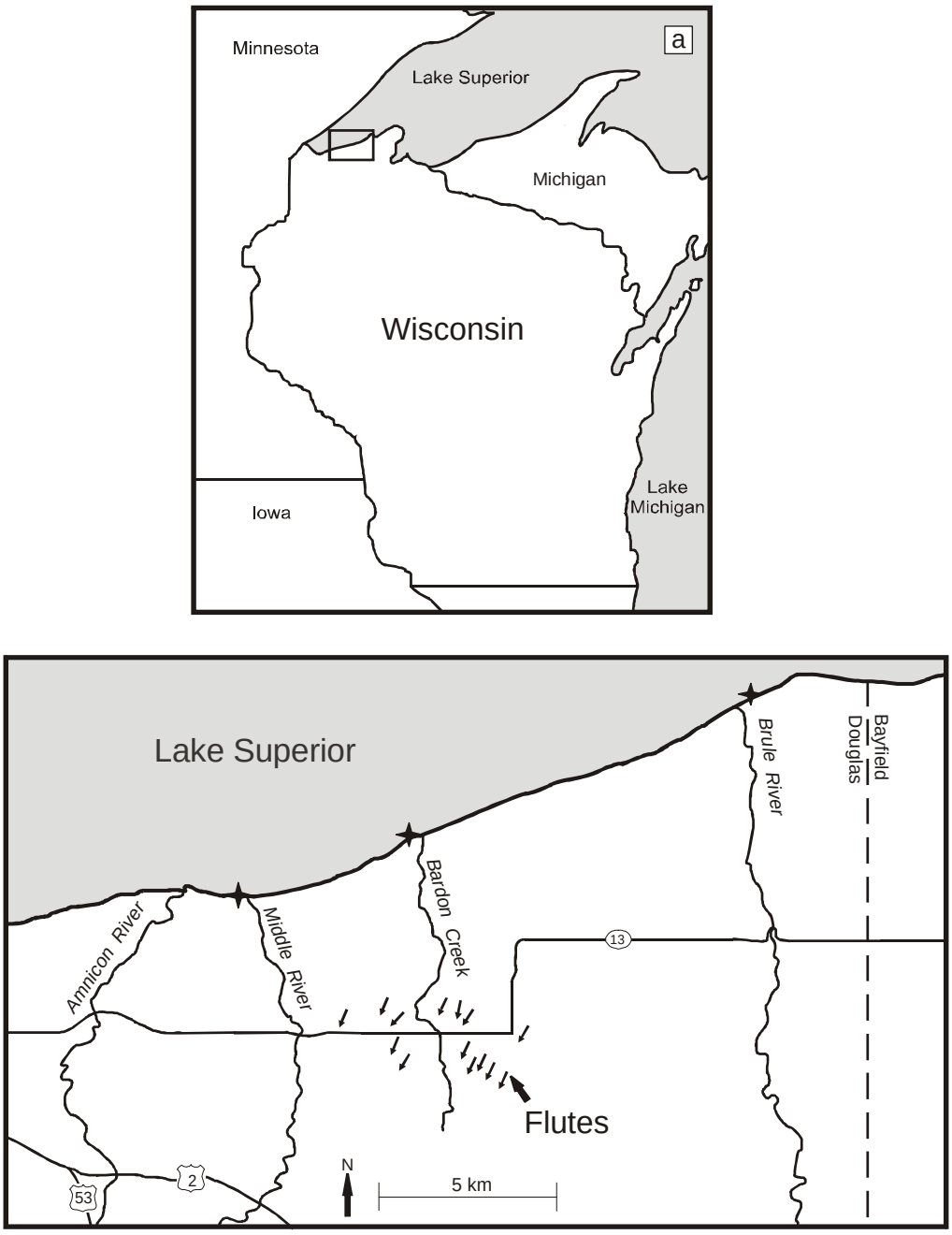

Figure 2.1. (a) Study site in northwestern Wisconsin. (b) Locations of sample profiles in northern Douglas County, Wisconsin. Stars mark locations of profiles.

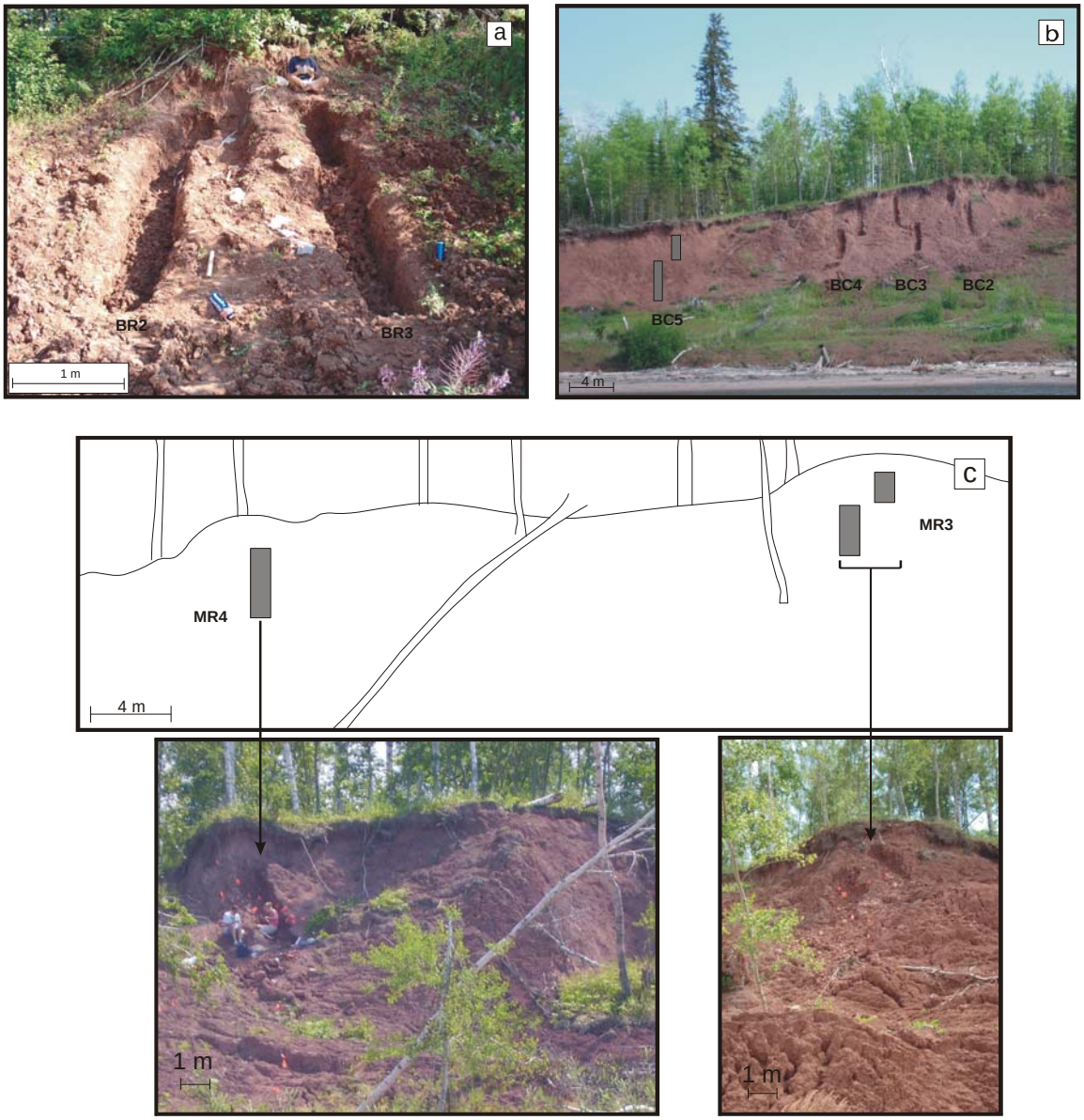

Figure 2.2. Profiles from each site sampled. (a) Brule River (BR), (b) Bardon Creek (BC), (c) Middle River (MR) (see Figure 2.1b for locations). The orange flags that can be seen in some of the photographs are elevation markers.

slightly in each of the four profiles. At Middle River samples were collected from 13.2 m to 17.0 m above lake level, with the ranges also differing slightly in each profile. The maximum elevation sampled at each site was dictated by the position of the root line from vegetation growing on top of the bluff. At Bardon Creek and Middle River the profiles did not extend to lake level because the bottom half of the bluff was covered with slumped clay and vegetation; at Brule River the bottom of the profile extended to the beach of Lake Superior.

Samples were collected along each profile by digging a trench about 0.5 m to 1.0 m wide into the bluff face until undisturbed till was reached, which was indicated by its greater cohesiveness. This required removing up to 0.5 m of colluvium. The longer profiles (BC2-BC5, MR3) were staggered laterally about 0.8 m to 1.3 m, so that two people could transport colluvium downslope at one time and thereby collect samples simultaneously. Elevation above lake level was determined along the bluff face using a Jacob's staff and Brunton compass and marked every 1.0 m. The 1.0 m markers were used as references to measure 0.2 m intervals in each trench. At each 0.2 m marker a horizontal platform or bench was created in the undisturbed till by excavating and trimming with putty knives (Figure 2.3). Twenty-five AMS samples and two intact blocks of till for measuring sand-particle fabric and microshear orientations were collected from the surface of each bench.

AMS samples were collected by pressing the open side of plastic cubic boxes, ~18 mm on a side with 1 mm wall thicknesses, into the bench surfaces, and then excavating them and replacing the covers. Only the outer 2 mm of the samples were

Figure 2.3. Example of a sampling bench with AMS cubes. AMS cubes are marked with an arrow that is oriented pointing north.

likely disturbed by pressing the boxes into the bench surface (Tarling and Hrouda, 1993). Each box was marked with an arrow and oriented using a Brunton compass so that the arrow pointed north before being pressed into the bench surface (Figure 2.3). A total of 4,122 AMS samples were collected. Due to the relatively high clay content of the till, it was generally soft, and AMS samples were easy to collect. However, a small hole had to be drilled into the top of each cube, so that air could be released from the cube while it was being pressed into the till.

The intact blocks of till (at least 5 cm x 5 cm x 7 cm) were collected from each bench either by being pulled out along natural breaks or cracks in the till (till had a blocky texture due to its high clay content) or by being cut out using putty knives. At higher elevations in the profiles, the till naturally broke into smaller intact fragments (3 to 5 cm). As a result, larger intact blocks had to be cut out using putty knives, and these blocks were often composed of an aggregate of smaller intact fragments. This made

sampling difficult in some cases because the blocks would often crumble into fragments upon excavation. At lower elevations natural partings in the till were more widely spaced, so large intact blocks (up to 25 cm in length) were easily obtained. Block orientations were recorded before being excavated with an arrow pointing north. The blocks were then sealed in plastic wrap to prevent drying and transported back to the lab, where they could be prepared for making thin sections.

C. Sample preparation

No preparation was required for AMS samples after being collected from the field. They could be analyzed in the condition they were in when collected.

The intact till blocks that were collected for measuring sand-particle fabric and microshear orientations were prepared in the lab for making thin sections. This process included several steps (Thomason and Iverson, 2006). First, blocks about 20 mm thick, 70 mm long, and 50 mm wide, were cut from the original field sample and submerged in acetone during eight exchanges, each with a duration of four to six hours. Acetone removes water from the samples while minimizing disturbance of expansive clay minerals (Clark, 1988; Thomason and Iverson, 2006). After the acetone exchanges were completed, the blocks were impregnated with an epoxy resin (Spurr resin). The impregnation process included eight exchanges every 12 hours using mixtures of acetone and epoxy in systematically varying ratios (3:1, 2:2, 1:3, entirely epoxy). The purpose of diluting the epoxy with acetone was to initially lower the viscosity of the epoxy so that it would more easily penetrate the samples. Each acetone/epoxy ratio was used twice. Finally, the samples were cured by heating in an oven at approximately 70^{o}C. Large thin

sections (51 mm x 70 mm) about 30 microns thick were cut from the center of each impregnated block. Both horizontal and vertical thin sections were made.

D. Measurements

AMS measurements were made using two devices for measuring magnetic susceptibility, the KLY-2 Kappabridge at the University of Minnesota's Institute for Rock Magnetism and the KLY-3S Kappabridge at the University of Wisconsin's Department of Geology and Geophysics. The latter device was used during the final stages of the project due its greater automation and speed.

To measure AMS, each sample is subjected to a magnetic field of known strength (H) in several orientations. In response to the magnetic field, magnetic minerals in the sample will magnetize. The strength of magnetization (M) that results is characterized by the susceptibility (k), which is the constant of proportionality between H and M (see Tarling and Hrouda, 1993; Martin-Hernandez et al., 2004 for a review). Susceptibility varies with orientation because some mineral grains are easier to magnetize in certain orientations. This anisotropy of susceptibility is best visualized with an ellipsoid, where the long, intermediate, and short axes represent maximum (k_1), intermediate (k_2), and minimum (k_3) susceptibilities, respectively (Figure 2.4).

AMS of samples can result from the preferred orientations of crystallographic axes (crystalline anisotropy) in minerals or from aligned non-equant grains (shape anisotropy). The source of anisotropy that is dominant depends on the type of magnetically susceptible minerals in the sample. When shape anisotropy is dominant, the direction of maximum susceptibility reflects the orientations of the long axes of grains

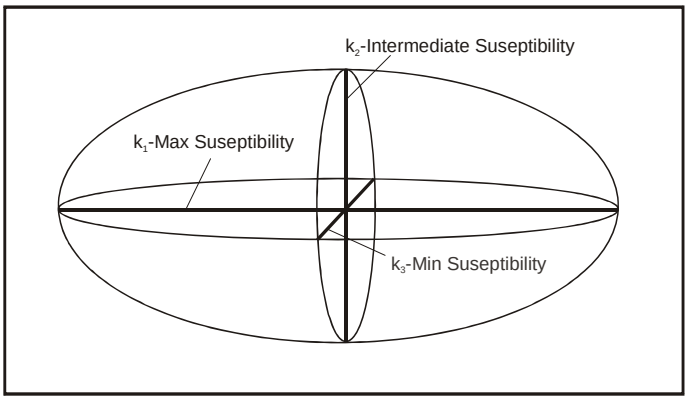

Figure 2.4. Susceptibility ellipsoid. An ellipsoid can be used to visualize the anisotropy of magnetic susceptibility of a sample. When non-equant magnetite grains are present, the induced magnetic field will be elongated in the preferred orientation of the long axes of magnetite grains (Tarling and Hrouda, 1993).

within the sample. In that case the orientation of k_1 can be used like the long axis of a single grain as a proxy for particle fabric. Magnetite is the dominant magnetic mineral in the Douglas till (Hooyer et al., in press), and is dominantly shape anisotropic. As a result, the direction of k_1 for the Douglas till reflects the orientation of non-equant magnetite particles (Hooyer et al., in press). Hysteresis experiments described by Hooyer et al. (in press) indicate that these particles are silt-sized or smaller.

Sand-particle fabric and microshear orientations were measured in thin sections using standard petrographic techniques (Thomason and Iverson, 2006). To measure sand-particle fabrics, digital photomicrographs (2x resolution) were taken at five to six random positions on each thin-section, and the orientation of all elongate particles ≥ 0.1 mm in length and with minimum axial ratios of 1.5 were measured (Figure 2.5a). A similar technique was used to measure the orientation of microshears, which are seen as birefringent lineaments under cross-polarized light (Figure 2.5b and c). However, microshears were not visible everywhere, so the locations of these measurements

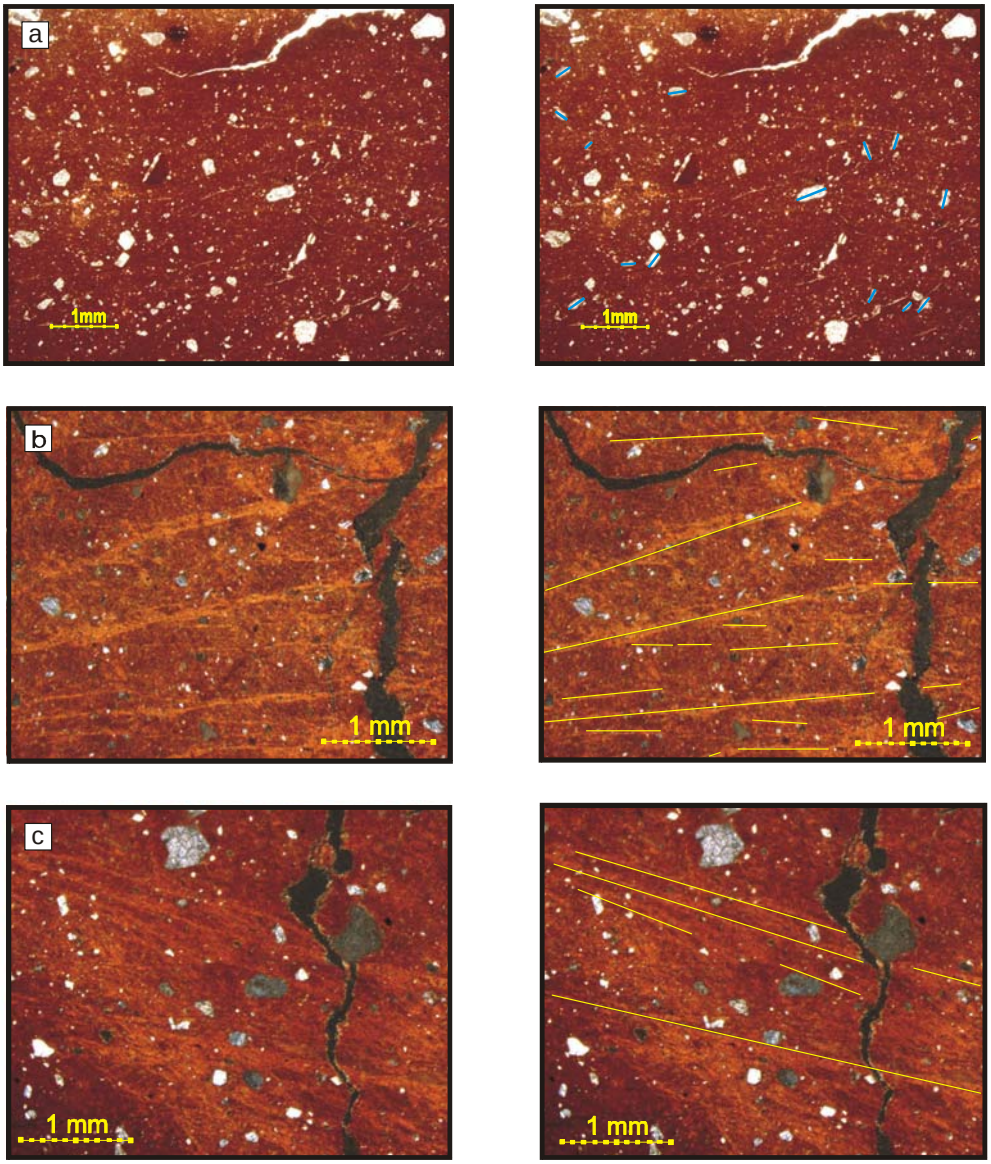

Figure 2.5. Examples of thin sections in which sand-particle and microshear orientations were measured. Right-hand column shows duplicate photomicrographs with the (a) long axes of sand grains traced with blue lines and (b) and (c) microshears traced with yellow lines. Photos in (a) were taken in plane-polarized light and photos in (b) and (c) were taken in cross-polarized light.

were not random. All orientation measurements were made using public-domain NIH Image software.

Thin sections were prepared in a two-step process. Horizontal thin sections were made and analyzed first to determine the preferred orientation (azimuth) of the long axis of grains. Vertical thin sections were then cut parallel to that orientation. If the sand-grain orientations were not clustered significantly around a preferred orientation, vertical thin sections were instead cut parallel to the regional ice-flow direction (N30^{o}E), as indicated by the trend of nearby flutes (Figure 2.1b). Sand-particle measurements were made for only the most vertically extensive profile (BC2), due to the expense and time required to impregnate till and make thin sections. Also, microshears were measured in only 12 thin sections from that profile because microshears could not be seen in all of the thin sections, perhaps due to spatial variations in their degree of impregnation or thickness.

E. Data presentation and analysis

AMS k_1 data were plotted on lower-hemisphere, equal-area stereonets, and sand-particle and microshear data were plotted on rose diagrams for each bench sampled. Fabric strength and direction were evaluated using the eigenvalue method of Mark (1973). For AMS the preferred orientation of k_1 is represented by an eigenvector (V_1), and the degree to which all k_1 orientations cluster around V_1 is described by an eigenvalue (S_1). $S_1 = 1.0$ reflects perfect alignment and $S_1 = 0.33$ reflects no alignment (isotropic distribution of orientations). The same technique was applied for sand-particle fabric, but the orientations of the long axes of grains were used to determine V_1 and S_1.

In the case of sand-particle fabric, $S_1 = 1.0$ reflects perfect alignment, but an isotropic fabric corresponds to $S_1 = 0.50$. This is because sand-particle data were obtained from thin sections and hence were two dimensional. The same technique was used for microshears, which were also measured in two dimensions.

F. Interpretation

Interpretations were grounded on results from ring-shear experiments that had been previously conducted using the Douglas till (Thomason and Iverson, 2006; Hooyer et al., in press). In these experiments, the Douglas till was sheared to strains as high as 714, and sand-particle fabric, microshear orientations (Thomason and Iverson, 2006), and AMS fabric (Hooyer et al., in press; Iverson et al., in press) were measured with increasing shear strain. The goal of these experiments was to study the progressive development of fabric with shear strain. Results indicated that sand-particle and AMS fabric development is similar. With increasing shear strain, strong flow-parallel fabrics developed and reached a steady state at strains between 7 and 39 for sand particles (Thomason and Iverson, 2006), and 6 and 25 for AMS (Hooyer et al., in press). For sand particles, the steady state S_1 value was ~0.72 (Figure 2.6a), and for AMS the steady state S_1 value was ~0.83 (Figure 2.6b). In addition, there was no clear tendency for fabric strength to weaken even at very high strains or become transverse to the shearing direction, contrary to theory developed for viscous fluids (Jeffery, 1922). Fabrics also plunged in the "upglacier" direction. Results also indicated that microshears became more pervasive and parallel to the shear plane as strain increased. At low shear strains, two sets of conjugate shears called Riedel shears (R_1 and R_2) developed at predictable

angles to the shearing direction (~25° and ~75°, respectively), which accommodated all deformation in the till (Figure 1.2). These shears dipped down-glacier. At higher strains (>10), lower-angle shears became more prominent.

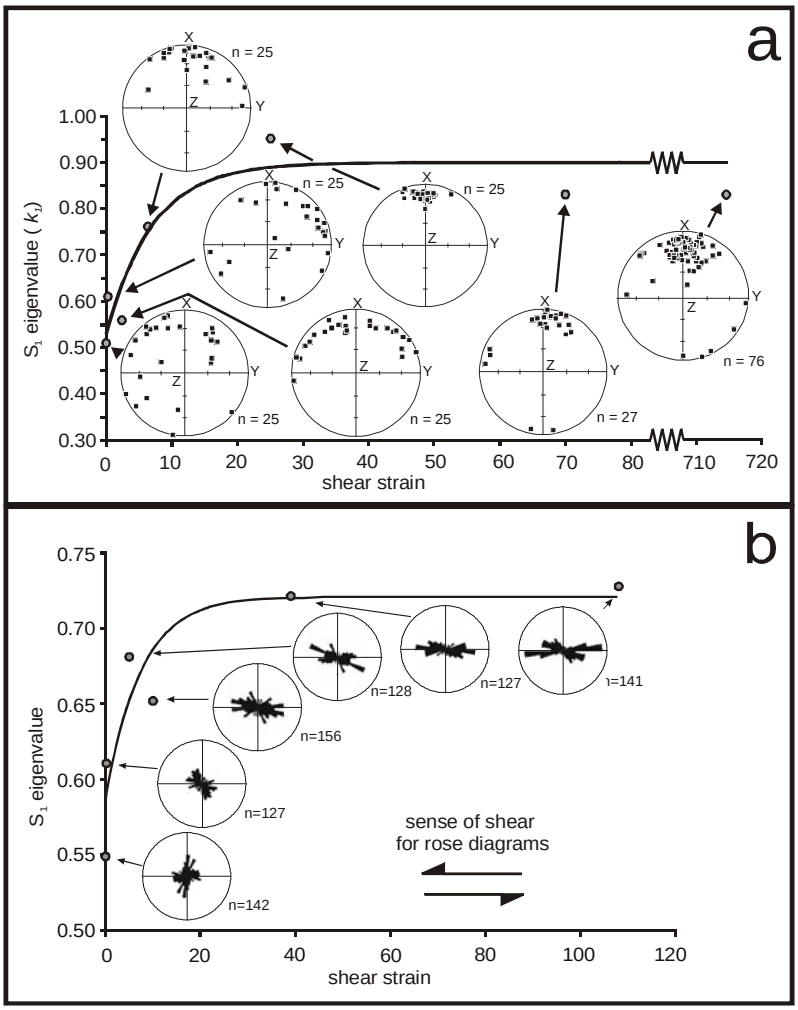

Figure 2.6. Results from ring shear experiments for Douglas till showing fabric development as a function of shear-strain magnitude. (a) AMS k_1 fabric with associated lower-hemisphere, equal-area stereonets. The value of n equals the number of samples measured for each experiment. Uncertainty of the shear strain values is ± 5%, and the standard error of the regression line is 0.063. The direction of shearing is along the x axis, and the sense of shear is bottom up, top down (from Hooyer et al., in press). (b) Sand-particle fabric measured from vertical, shear parallel planes with associated rose diagrams. The value of n is equal to the number of particles measured for each experiment. The radius of each rose diagram represents 40 particles. Uncertainty of the shear strain values is ± 5%, and the standard error for the regression line is 0.032 (from Thomason and Iverson, 2006).

CHAPTER 3. RESULTS

A. AMS vs. sand-particle fabric

Only in profile BC2 at Bardon Creek were both AMS and sand-particle fabrics measured. In general, AMS and sand-particle analyses give rise to similar V_1 azimuths (Figure 3.1). A coefficient of determination (r^2) of 0.60 for the regression between AMS V_1 azimuths and sand-particle V_1 azimuths demonstrates this similarity (Figure 3.2)[1]. Samples with low S_1 values (45%) were not included in this regression because V_1 correlations are significant only when S_1 values indicate significant clustering; $S_1 = 0.58$ was chosen arbitrarily as the threshold value. AMS S_1 values are consistently larger than sand-particle S_1 values. However, as noted by Thomason and Iverson (2006), because a single k_1 orientation depends on the alignment of many magnetically susceptible particles, as well as on their magnetic mineralogy, comparisons of S_1 values based on k_1 and particle fabrics is not meaningful. AMS provides more useful data than sand particles because AMS fabrics are three-dimensional and their measurement involves less human subjectivity than the measurement of individual sand grains in thin section. In addition, a single k_1 azimuth reflects the volume-averaged orientation of many magnetically susceptible particles in a sample cube. As a result, the inherent variability of k_1 orientations is less than that of individual particle orientations (Thomason, 2006; Hooyer et al., in press; Iverson et al., in press). Therefore, AMS data were the focus of the other profiles.

[1] This regression also includes some preliminary data that were not discussed in the Methods section.

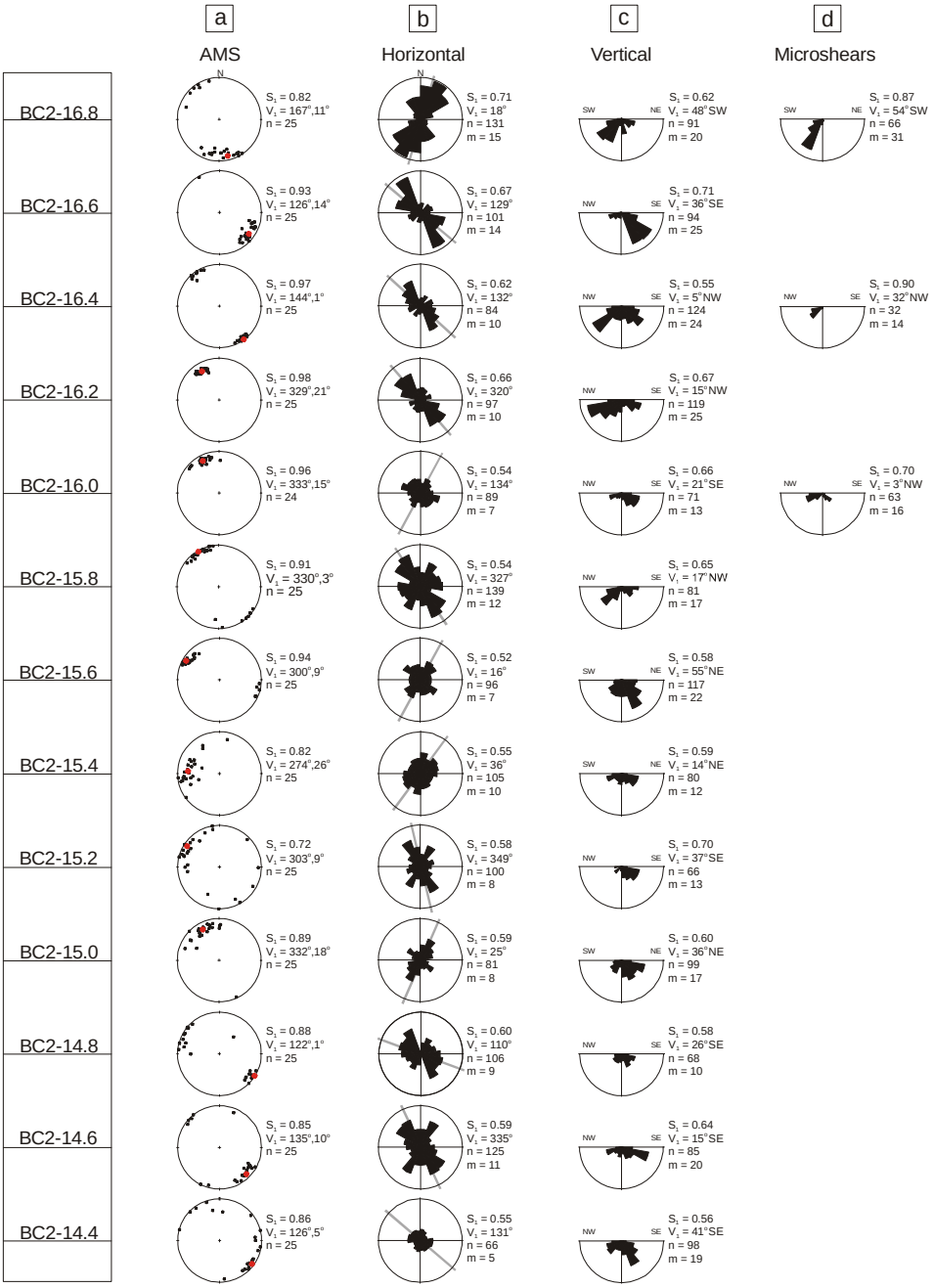

Figure 3.1. AMS, sand-particle, and microshear data from profile BC2 at Bardon Creek. BC2-# indicates the elevation above lake level (m). (a) Stereoplots with directions of maximum magnetic susceptibility (k_1). Red dots are eigenvectors. (b) Rose diagrams with sand-particle orientations measured in a horizontal plane. Gray lines indicate the orientations of vertical thin sections. Outer edge of plots equals 15 grains. (c) Rose diagrams with sand-particle orientations measured in vertical planes. Outer edge of half-circle equals 30 grains. (d) Rose diagrams with microshear orientations measured in vertical planes. Outer edge of half-circle equals 40 microshears.

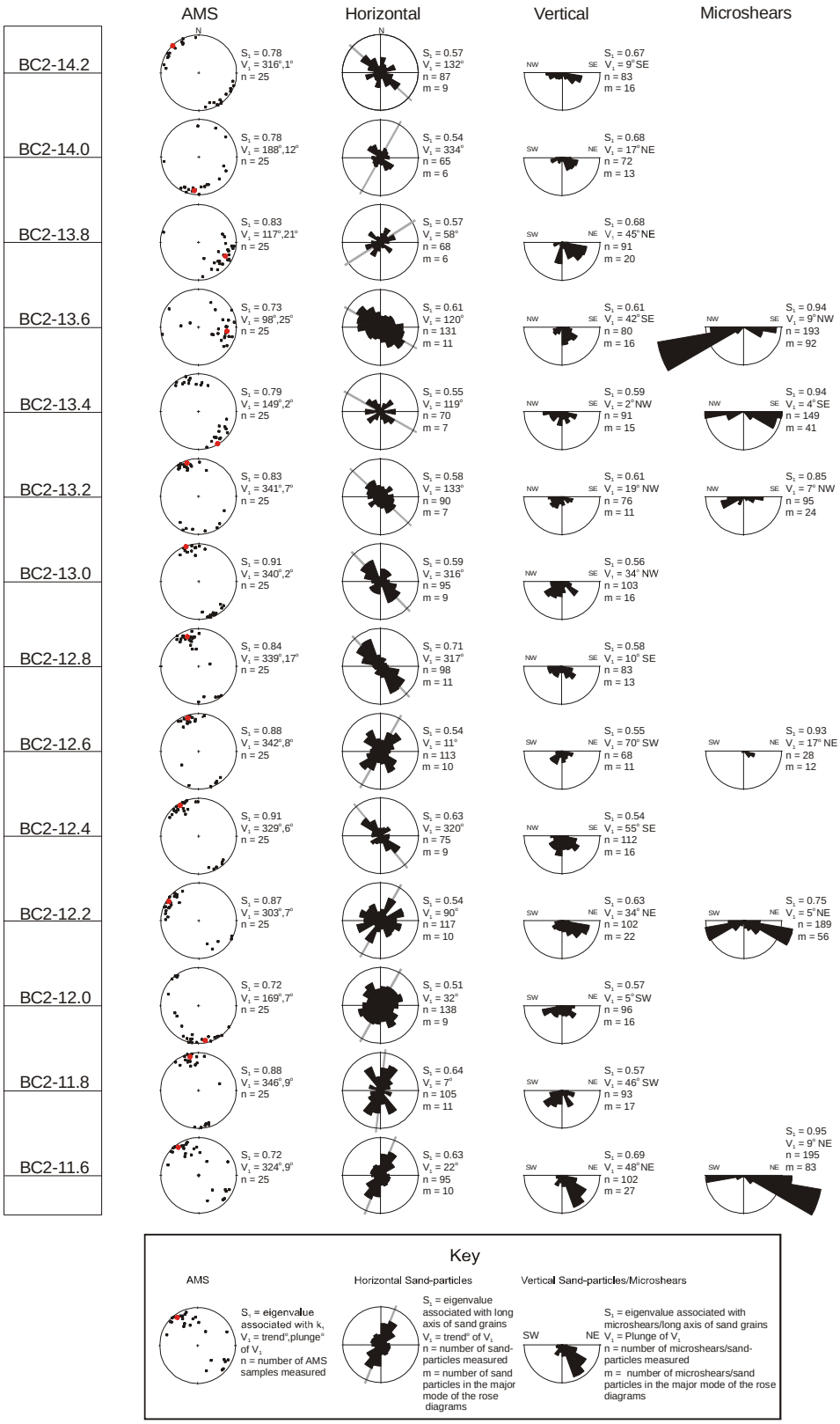

Figure 3.1. (continued)

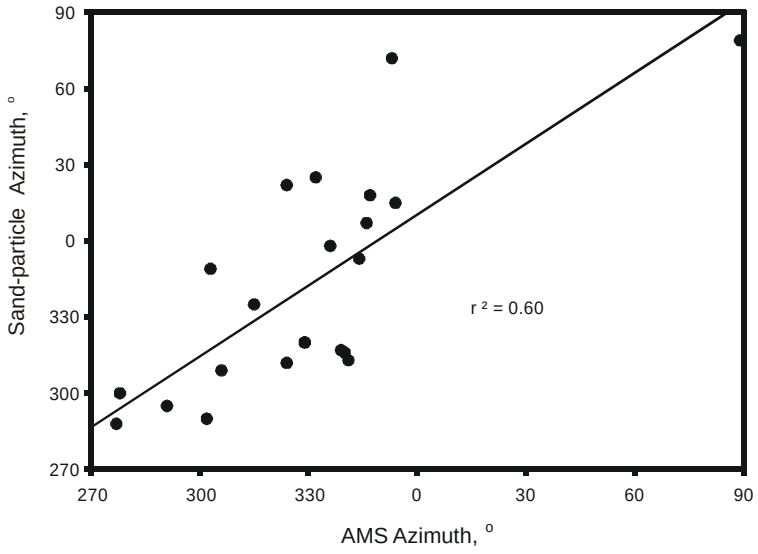

Figure 3.2. Comparison of AMS and sand-particle fabric azimuths from profile BC2 (also includes some preliminary data not discussed in the Methods section). All V_1 orientations with S_1 eigenvalues less than 0.58 were not included in the regression. Zero degrees is north with degrees increasing clockwise (90^o is east and 270^o is west).

B. S_1 values with depth

At Bardon Creek, AMS S_1 values vary with depth but are generally large (Figure 3.3). In fact, ~ 57% of the fabrics are as strong as or stronger than the steady-state strength attained at moderate shear strains (~20) in ring-shear experiments using the Douglas till ($S_1 = 0.83$). In some sections of the profiles, fabrics are consistently very strong ($S_1 > 0.90$). For example, in BC4 from 13.2 m to 14.6 m above lake level S_1 values exceed 0.90 (Figure 3.3).

At the two other outcrops located down the shoreline to the east and west, results were similar. At Brule River, S_1 values also vary with depth but are generally large (Figure 3.4). About 80% are as large as or larger than the steady-state value from ring-shear experiments. Fabrics in BR3 are consistently stronger than the steady-state

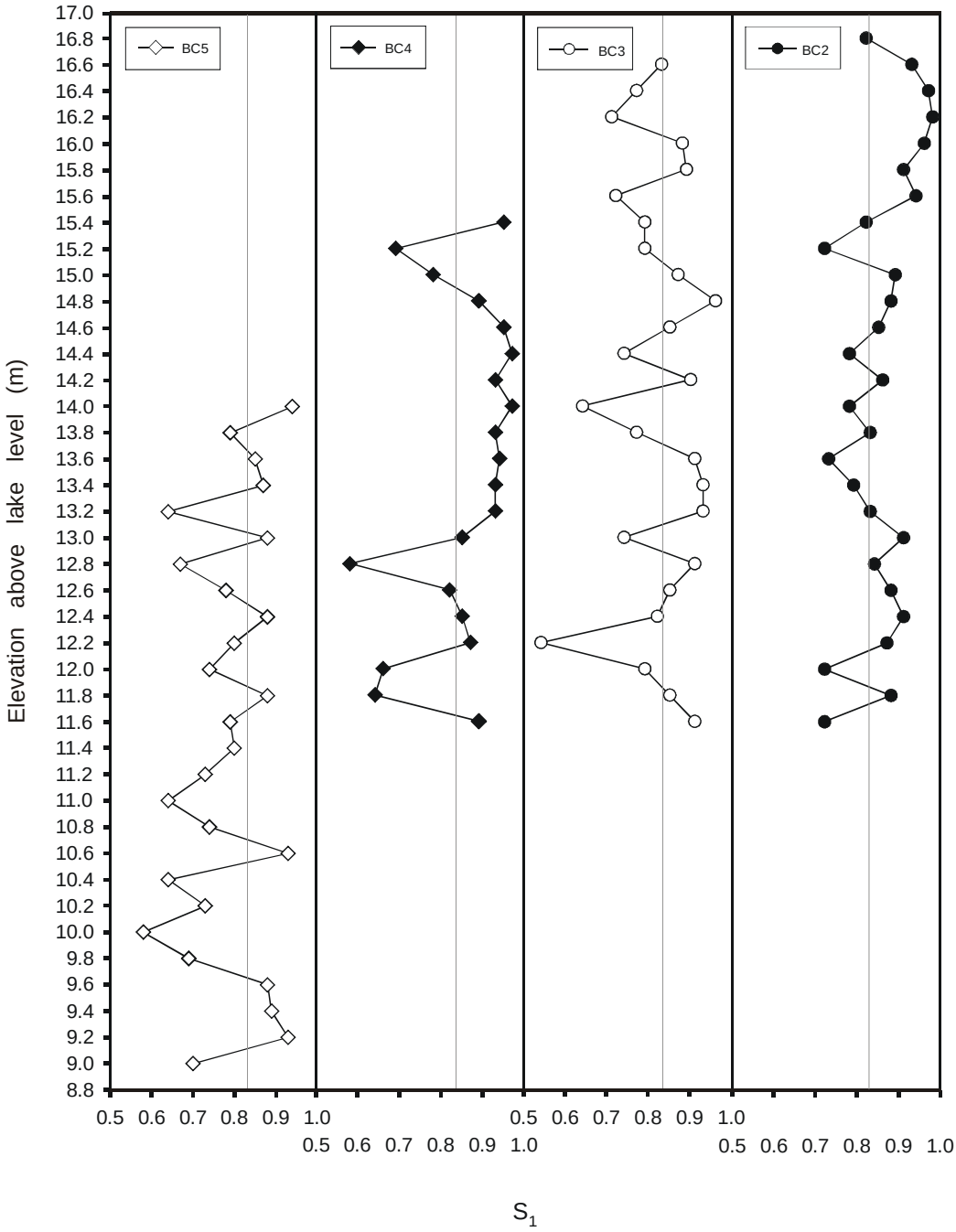

Figure 3.3. AMS fabric strength (S_1 eigenvalues) within profiles at Bardon Creek (BC). The grey lines in each plot represent the steady-state eigenvalue from ring-shear experiments with the Douglas till ($S_1 = 0.83$).

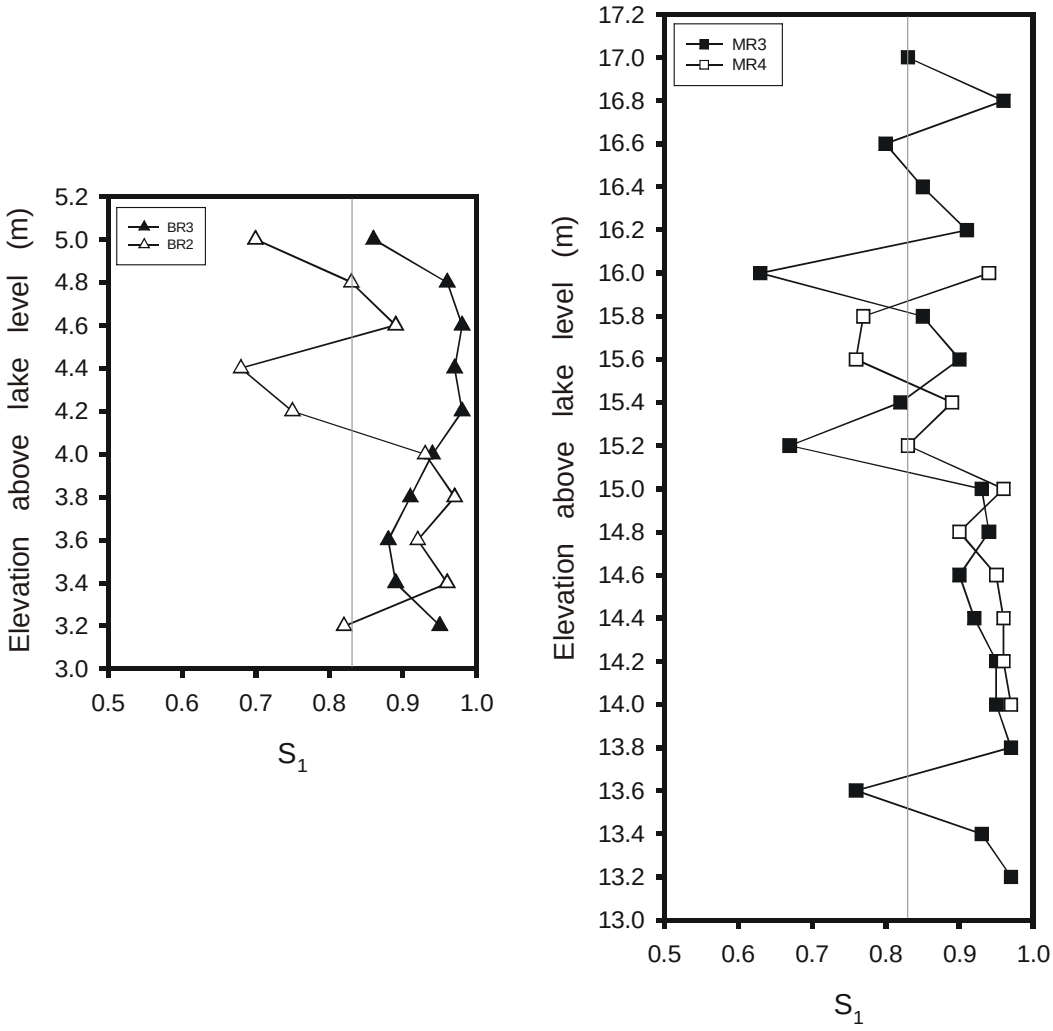

Figure 3.4. AMS fabric strength (S_1 eigenvalues) within profiles at Brule River (BR) and Middle River (MR). The grey lines in each plot represent the steady-state eigenvalue from ring-shear experiments with the Douglas till ($S_1 = 0.83$).

strength whereas BR2 fabric strengths vary more with depth. At Middle River, ~77% of the fabrics are as strong as or stronger than the steady-state strength from ring-shear experiments. Striking aspects of the data from Middle River are the uniformly strong fabrics from 13.8 m to 15.0 m in both MR3 and MR4 ($S_1 > 0.90$) (Figure 3.4).

C. V_1 orientations with depth

Similar to S_1 values, V_1 orientations also vary with depth at Bardon Creek (Figure 3.5). In profiles BC2 and BC3, V_1 azimuths are generally transverse to the regional ice-flow direction (N30^{o}E), taken to be parallel to the flutes nearby (Figure 2.1b). In contrast, V_1 azimuths in BC4 are generally parallel to the regional ice-flow direction. This is an interesting result because BC3 and BC4 are within 6 m of one another on the bluff face. V_1 azimuths in BC5 vary more abruptly from one depth to another, in some places changing from fully transverse to flow-parallel over one sampling interval (0.2 m). An important observation from Bardon Creek is the uniformly flow-parallel fabric in BC4 from 12.8 m to 15.2 m (Figure 3.5; also see appendix Figure A3). There are also sections with relatively uniform V_1 azimuths in BC2 from 12.6 m to 13.2 m and from 15.8 m to 16.4 m, in BC3 from 13.4 to 13.8 m, and in BC5 from 13.2 m to 13.6 m.

At Brule River and Middle River, V_1 orientations similarly either vary with depth (Figure 3.6) or are uniformly parallel to the regional ice-flow direction. In the Brule River profiles, azimuths are generally parallel to the regional ice-flow direction, with the exception of azimuths at a few elevations in BR2 that deviate from the flute direction substantially. Azimuths in BR3 are strikingly uniform and parallel to the regional flow direction throughout the profile. Middle River azimuths appear to change more smoothly

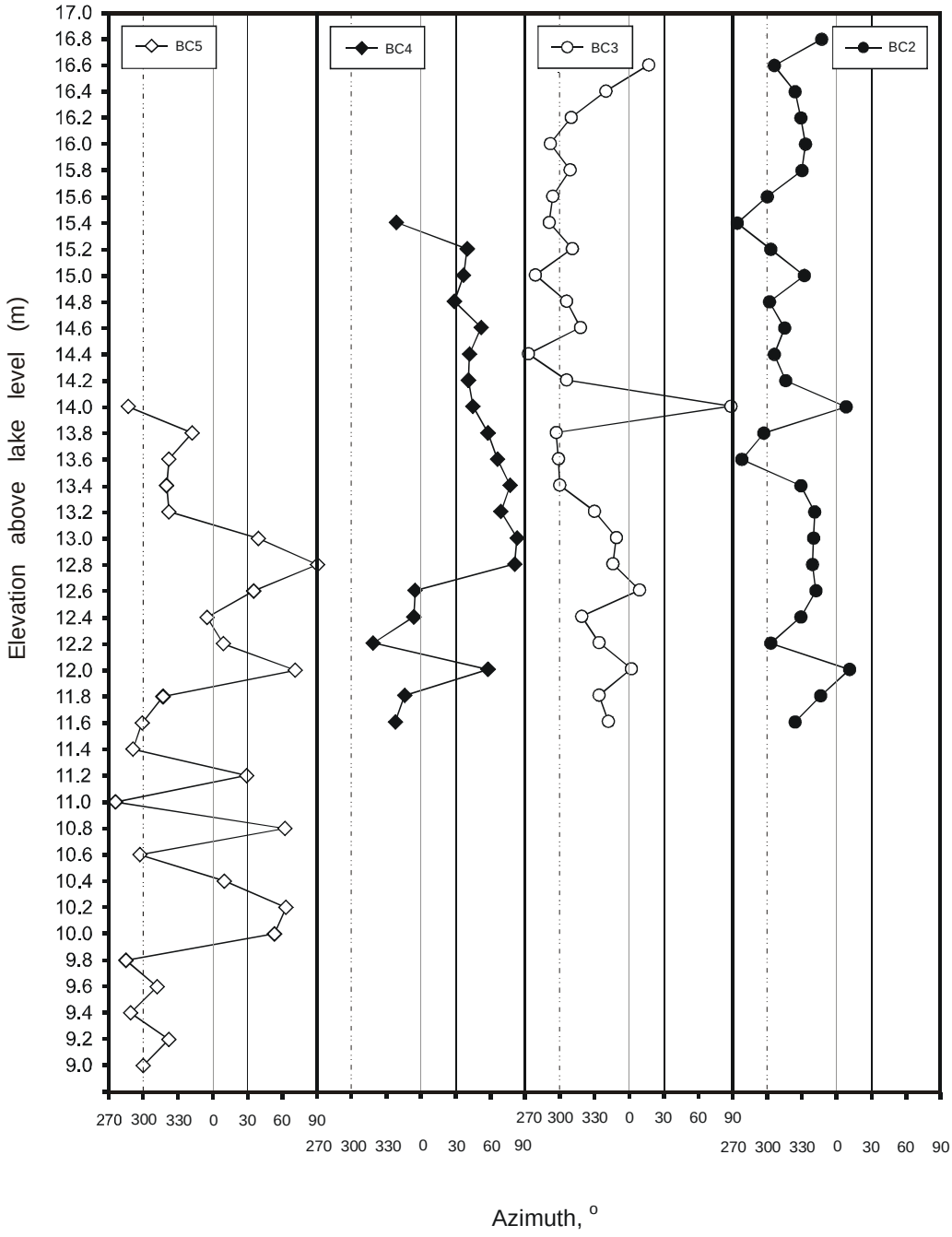

Figure 3.5. AMS fabric azimuths (V_1 orientations) within profiles at Bardon Creek (BC). The grey lines represent north, the solid black lines represent flute orientations near the study area (taken to be parallel to regional ice-flow direction), and the dashed/dotted lines represent the direction transverse to the regional ice-flow direction in each plot. Zero degrees is north with degrees increasing clockwise (90° is east and 270° is west).

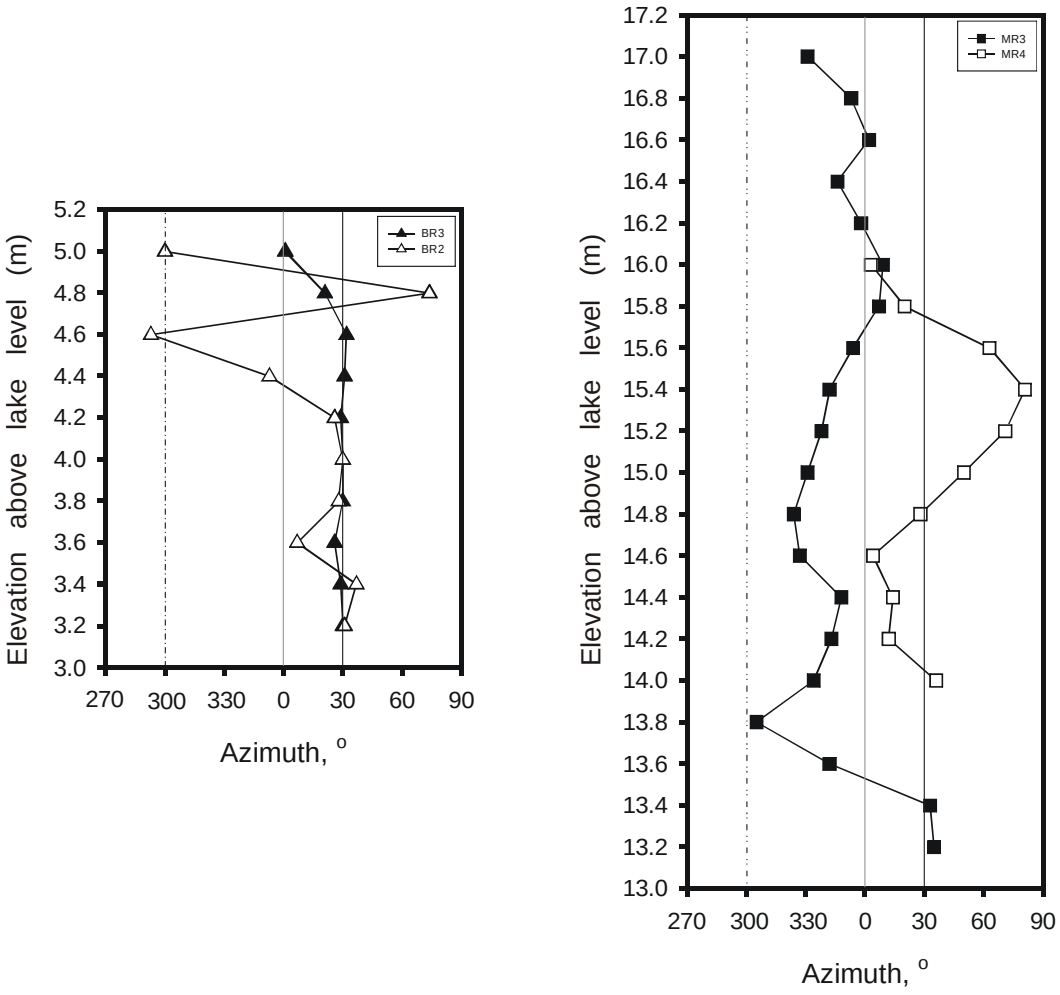

Figure 3.6. AMS fabric azimuths (V_1 orientation) within profiles at Brule River (BR) and Middle River (MR). The grey lines represent north, the solid black lines represent flute orientations near the study area (taken to be parallel to regional ice-flow direction), and the dashed/dotted lines represent the direction transverse to the regional ice-flow direction in each plot. Zero degrees is north with degrees increasing clockwise (90^o is east and 270^o is west).

with depth than at Bardon Creek and Brule River. In MR3, V_1 azimuths vary smoothly through orientations that lie between transverse and parallel to the regional ice-flow direction. In contrast, MR4 V_1 azimuths tend to vary about the regional ice-flow direction.

D. Fabric plunge directions

Plunge directions of AMS fabrics parallel and transverse to the regional flow direction, as indicated by the flute orientation, are considered separately. Plunge directions of fabrics roughly parallel to the flute direction vary with depth but are dominantly to the northeast (79%) (Figures 3.7 and 3.8). The only significant deviation is in a one meter section of MR4 (14.6-16.6 m above lake level) in which fabrics plunge uniformly to the southwest (Figure 3.8). Fabrics oriented roughly perpendicular to the flute direction show some tendency to plunge to the northwest (66%) (Figure 3.9 and 3.10). This tendency is particularly strong in profiles BC4 (Figure 3.9) and MR3 (Figure 3.10) where all transverse fabrics plunge to the northwest, but in all profiles where there are more than three transverse orientations there is a greater tendency for fabrics to plunge to the northwest rather than to the southeast.

E. Is variability in V_1 orientation with depth significant?

One way to assess if the variability in V_1 azimuth with depth is significant is to plot V_1 orientations from each elevation in a given profile on a stereoplot and determine the associated S_1 eigenvalue. If the S_1 eigenvalue associated with V_1 azimuths falls within the standard deviation of the average S_1 value for the entire profile, the variability in V_1 azimuth with depth is not significant. In that case, any apparent variability in V_1

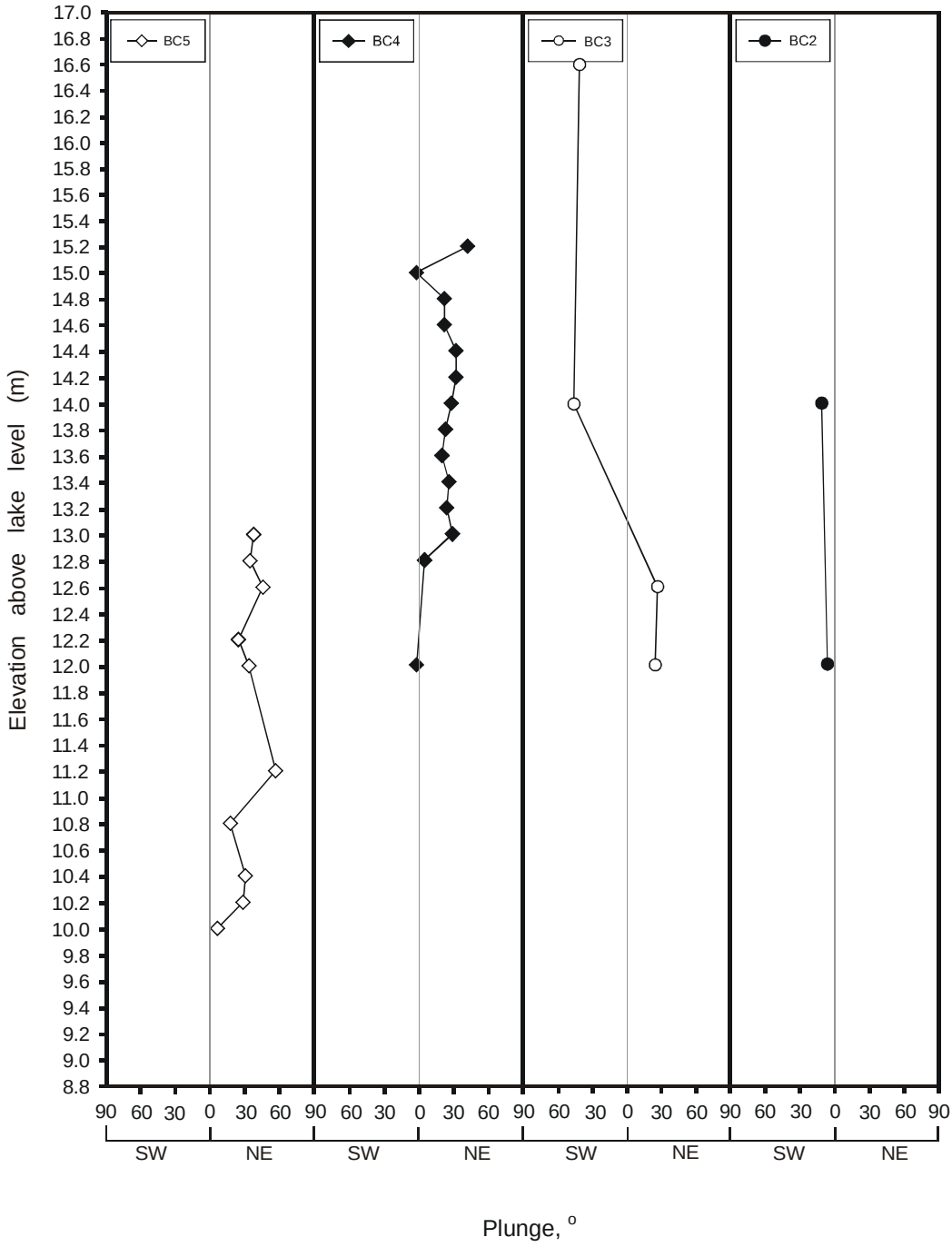

Figure 3.7. AMS plunges (V_1) of flow-parallel fabrics within profiles at Bardon Creek (BC). The grey lines indicate zero plunge.

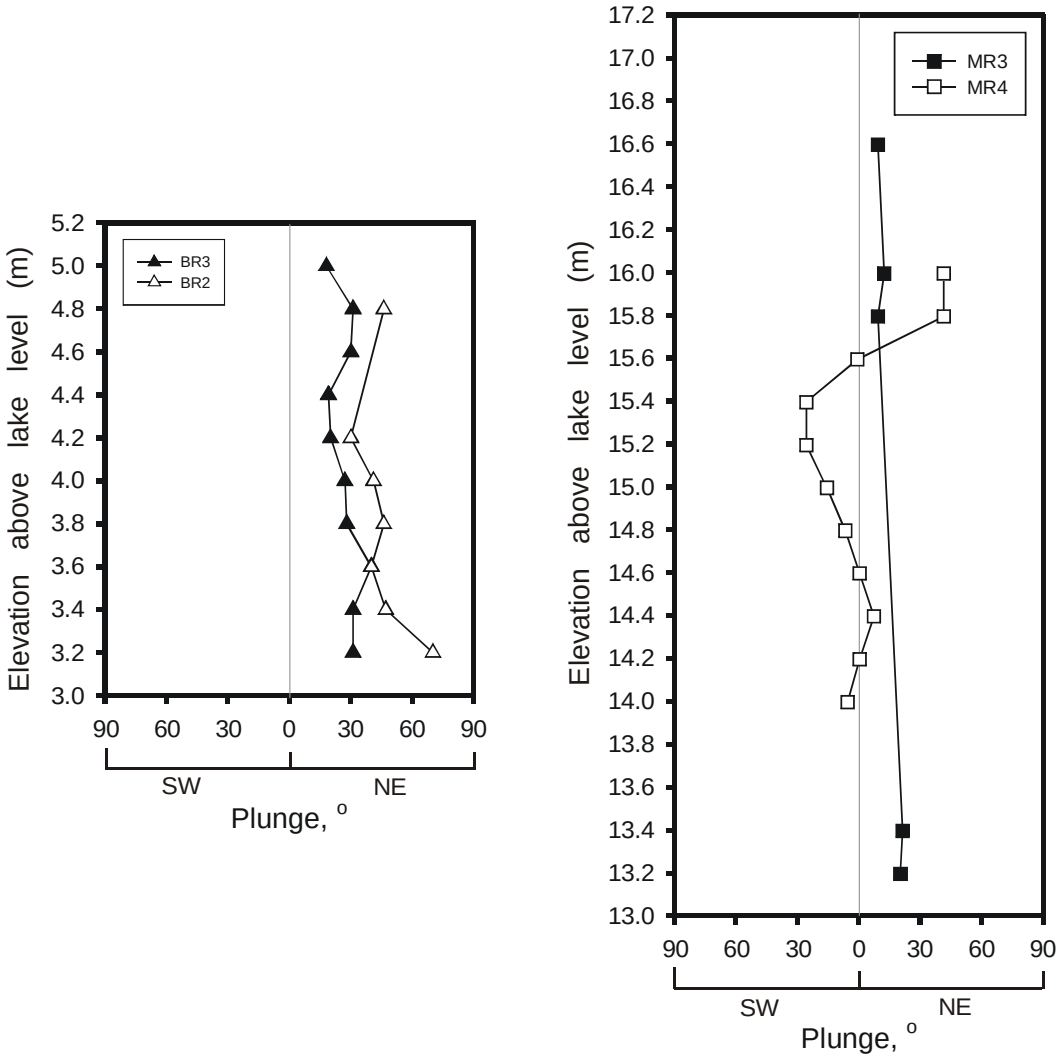

Figure 3.8. AMS plunges (V_1) of flow-parallel fabrics within profiles at Brule River (BR) and Middle River (MR). The grey lines indicate zero plunge.

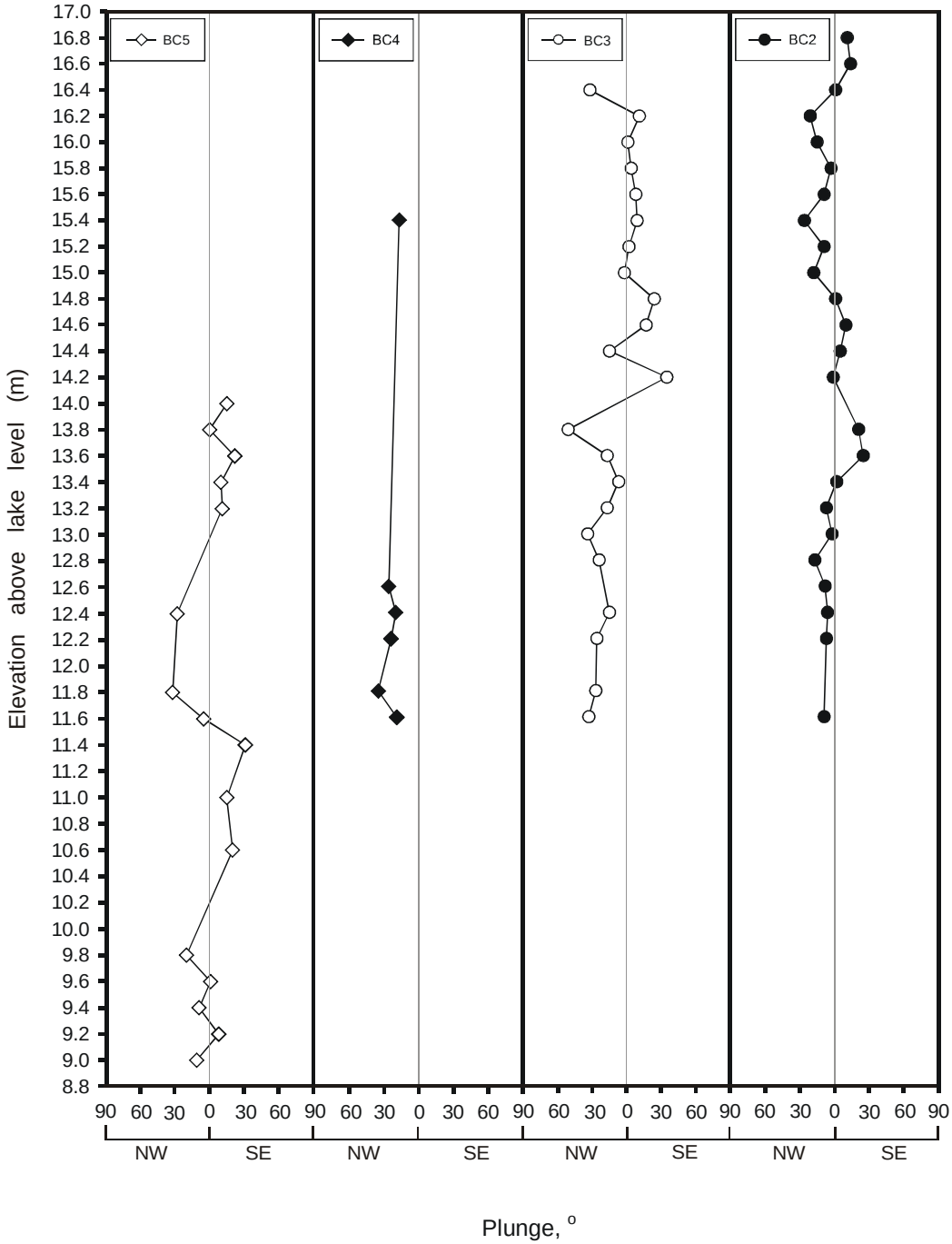

Figure 3.9. AMS plunges (V_1) of transverse fabrics within profiles at Bardon Creek (BC). The grey lines indicate zero plunge.

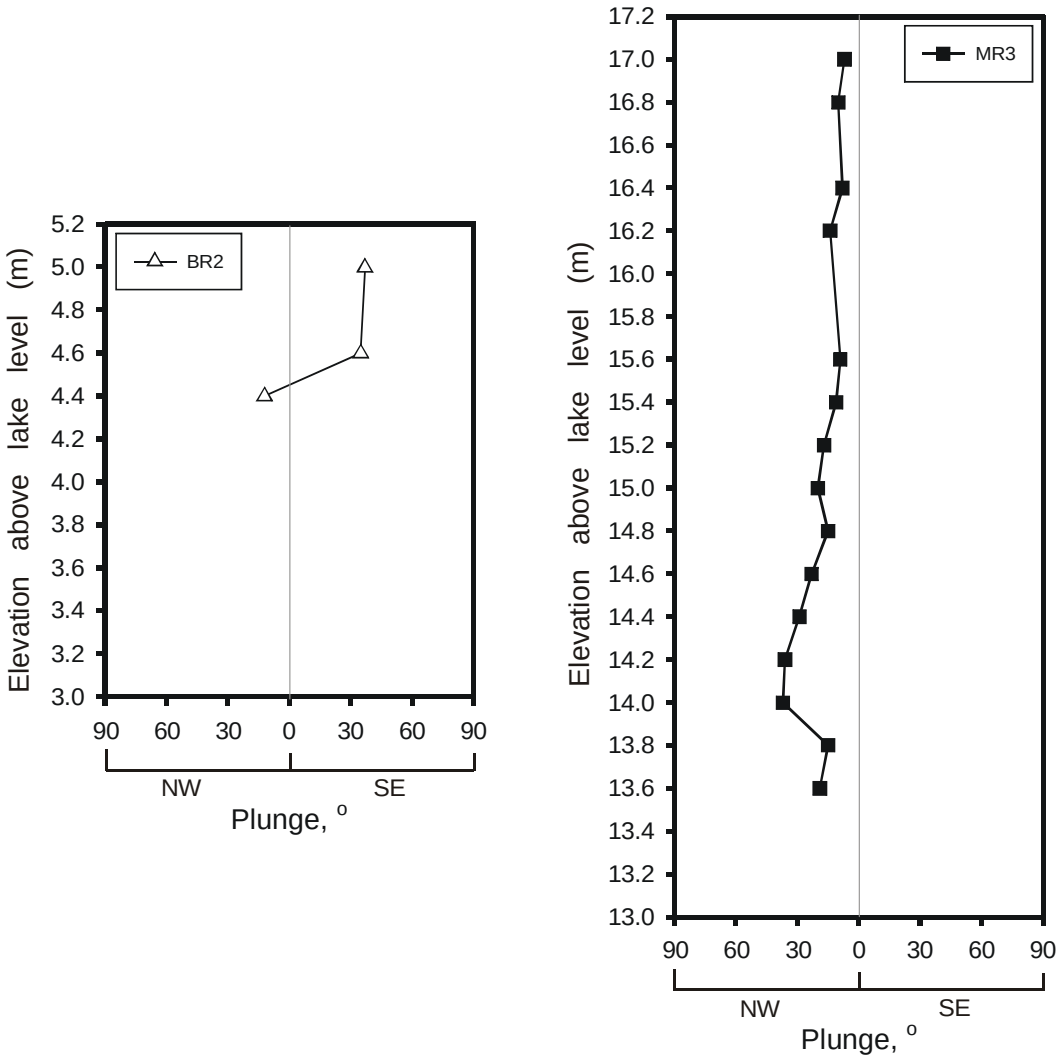

Figure 3.10. AMS plunges (V_1) of transverse fabrics within profiles at Brule River (BR) and Middle River (MR). The grey lines indicate zero plunge.

azimuth is most likely noise because the variability with depth is less than or equal to the variability at any given elevation in the profile. However, if the S_1 value associated with the V_1 orientations in a profile does not fall within the standard deviation of the average S_1 value in the profile, the variability in V_1 with depth can be considered significant. Results analyzed using this criterion indicate that variability in azimuth with depth is not significant in profiles BC2, BR3, and MR3 and is significant in profiles BC3, BC4, BC5, BR2, and MR4 (Figure 3.11).

F. Microshears

Microshears that were measured in thin sections from BC2 typically plunge gently (3^o to 32^o), with the exception of at 16.8 m above lake level where they plunge more steeply (54^o) (Figure 3.1). The direction of plunge is less systematic, but microshears have a tendency to dip either to the northwest or northeast. This is true in seven out of the ten thin sections that contained discernable microshears. The degree to which microshear orientations at a given elevation cluster is generally high, with S_1 eigenvalues between 0.70 and 0.99.

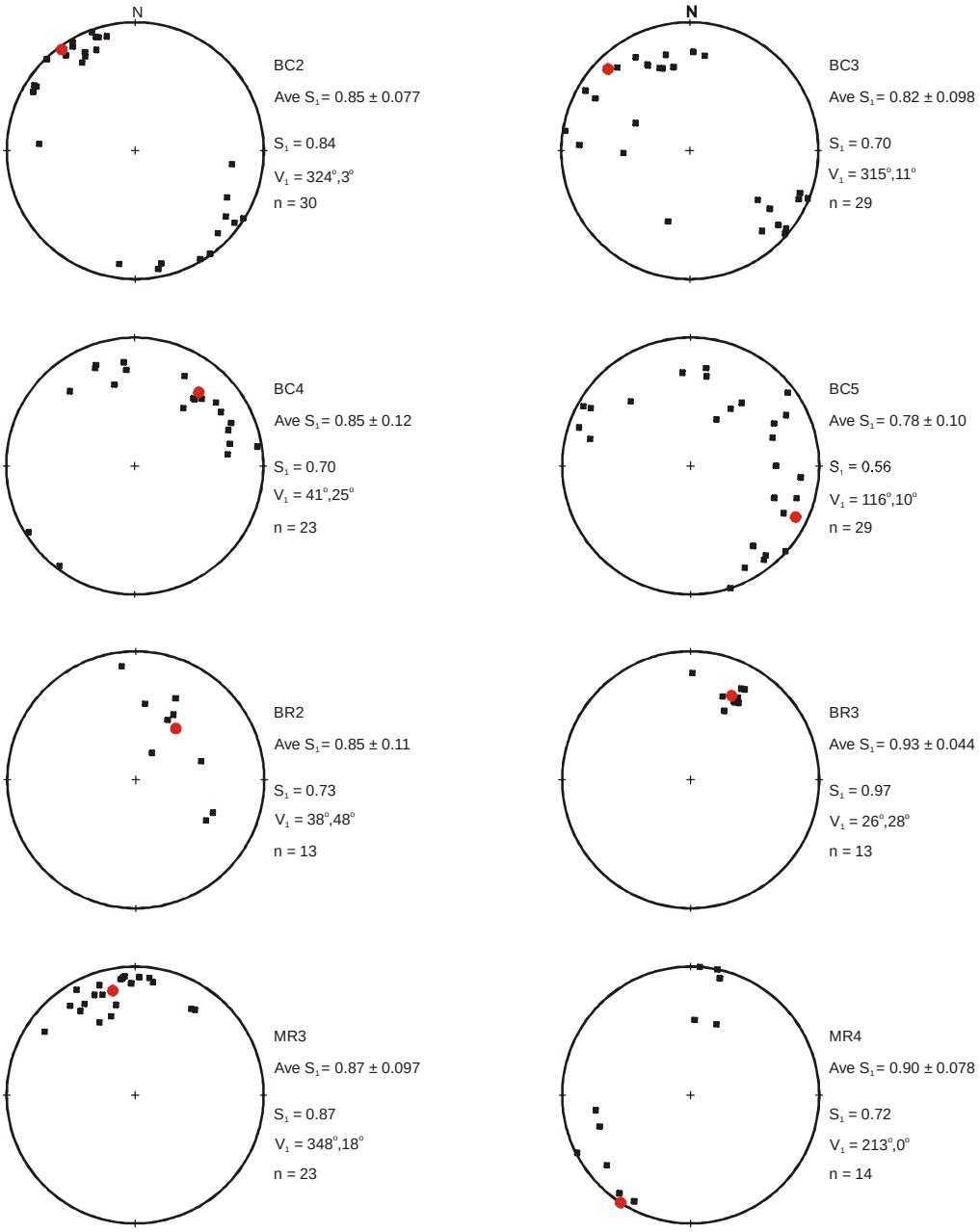

Figure 3.11. Stereoplots indicating significance of depth variability of fabric directions, with AMS V_1 orientations plotted for each profile. Ave S_1 is the average S_1 value for each profile ± the standard deviation. S_1 is the value associated with V_1 orientations for each plot, and V_1 is the trend and plunge of the V_1 eigenvector associated with the AMS V_1 orientations for each profile. The variable n is the number of data points plotted. If S_1 falls within the standard deviation of the Ave S_1 variability, depth variability of fabric direction is considered insignificant.

CHAPTER 4. DISCUSSION

A. Confirmation that the Douglas member is till

One goal of this study was to evaluate Johnson's (1980; 1983) conclusion that the Douglas member consists of till rather than lake sediment. Results from this study do, in fact, support this conclusion. Strong, unimodal fabrics measured in the Douglas member indicate that shear deformation occurred, which resulted in the alignment of particles. Either debris-laden basal ice was sheared, with subsequent deposition of sediment by melt-out and preservation of particle fabrics (Lawson, 1979), or subglacial sediment was sheared during lodgement or deeper deformation of the bed (Thomason and Iverson, 2006; Hooyer et al., in press). The presence of microshears in the Douglas member indicates that fabric likely developed during subglacial shear because microshears are not expected to form during viscous deformation of ice, even if ice contains debris (Thomason and Iverson, 2006). However, the possibility that the microshears are related to post-glacial shrinking and swelling of clay minerals cannot be ruled out.

If the Douglas member was undisturbed lake sediment, it would most likely exhibit girdle-shaped fabrics rather than unimodal clusters. This is because clay and silt-sized particles that settle to the bottom of a lake will deposit sub-horizontally but with no preferred azimuth (Hamilton and Rees, 1970; Tarling and Hrouda, 1993 pp. 98-99; Kissel et al., 1998; Park et al., 2000; Nowaczyk, 2003). Although the fabric of the Douglas member indicates glacial transport, its high clay content and conspicuous lack of gravel-sized and larger particles indicate that its protolith was probably lake sediment. This inference is also supported by mapping of the region surrounding the area spanned by the

Douglas member, which has shoreline deposits that mark the extent of former proglacial lakes (Johnson, 1983). If the protolith was indeed derived from a proglacial lake, the trend of becoming increasingly fine-grained to the west may be related to the proximity of deposition to the ice margin (Johnson, 1980)

B. AMS fabric vs. sand-particle fabric

An important result of this study is that AMS and sand-particle fabric analyses generally yield V_1 azimuths that are similar but not very strongly correlated (Figure 3.1). A coefficient of determination of 0.60 for the regression between AMS and sand-particle V_1 azimuths indicates that 60% of the variability of sand-particle fabrics could be predicted using AMS fabrics or vice versa (Figure 3.2). The fact that AMS and sand-particle V_1 azimuths do not correlate more closely may reflect a difference between the rotations of silt- and sand-sized particles during shear.

A more likely alternative, however, for the lack of a stronger correlation may reflect the signal-to-noise ratio of particle-fabric measurements, which is lower than that of AMS-fabric measurements. Fabric analyses that involve measuring the orientations of individual particles can have major sources of uncertainty due to human subjectivity (Drake, 1977; Benn and Ringrose, 2001; Klein and Davis, 2002). In contrast, there is very little human error during the collection and measurement of AMS samples (Hooyer et al., in press; Iverson et al., in press). Furthermore, measurement of an AMS sample reflects the volume-averaged orientation of many magnetically susceptible particles, rather than the orientation of a single grain, which means that the inherent variability of k_1 is less than that of a single sand-particle orientation (Hooyer et al., in press; Iverson et

al., in press). Sand-particle data are also limited to measurements in a plane, which can contribute to variability in sand-particle fabrics relative to fully three-dimensional AMS fabrics.

Nevertheless, the correlation between orientations of AMS and particle fabrics is important because it provides further support for use of AMS as a indicator of particle fabric and ultimately of strain magnitude and direction. Similarities between AMS and particle-fabric orientations have also been found in ring-shear experiments using till (Thomason and Iverson, 2006; Hooyer et al., in press; Iverson et al., in press) and in field studies of both fault gouge (Hayman et al., 2004) and till (Fuller, 1964; Stewart et al., 1988; Thomason, 2006). For example, Thomason (2006) determined a coefficient of determination of 0.55 for the correlation between AMS and sand-particle fabric azimuths for the Batestown till of the Lake Michigan lobe.

Unlike orientations of AMS and particle fabrics, strengths of AMS and particle fabrics cannot be meaningfully compared (Hooyer et al., in press); AMS k_1 orientation reflects both the volume-integrated alignment of many grains and the nature of their shape anisotropy. Thus, S_1 values based on clustering of k_1 orientations are not expected to be the same as those calculated from direct measurements of the orientations of individual particles of any size.

C. Strain magnitude of the Douglas till

Although the Douglas till has clearly been deformed, a key question is whether the Douglas till was sheared to the high strains (>100) required by the bed-deformation

model of glacier flow. In ring-shear experiments using the Douglas till, strong, flow-parallel AMS fabrics, with a steady state S_1 eigenvalue of 0.83, developed at a shear strain of ~20 (Fig. 2.6a). In addition, there was no tendency for fabric strength to weaken with increasing strain (Hooyer et al., in press; Iverson et al., in press). This means that the Douglas till should exhibit S_1 eigenvalues of at least 0.83 if it was deformed pervasively to a strain greater than ~20.

This direct comparison of laboratory and field S_1 values neglects the difference in fabrics prior to shearing in the field and laboratory. The girdle fabrics that are inferred to have characterized the lake-sediment protolith of the Douglas till likely required less strain to attain a steady-state clustered fabric than in the laboratory, where the initial S_1 values were smaller. However, this difference in strain required to reach a steady state was likely small; ring-shear experiments indicate that girdle fabrics develop at low strains (~1.0) and that most of the strain required to attain a steady-state fabric involves transformation of fabrics from girdles to clusters (Iverson et al., in press). Thus, the difference in strain required to attain a steady-state fabric in the field and laboratory was likely small.

Results from this study indicate that AMS fabrics in the Douglas till generally do have S_1 values that are ≥ 0.83 (Figures 3.3 and 3.4), which are sufficiently high for the bed-deformation model not to be ruled out. For the entire dataset, approximately 63% of S_1 values are ≥ 0.83, with S_1 values as high as 0.98 at two of the three sites sampled (Figures 3.3 and 3.4). However, the only conclusion that can be reached from S_1 values

> 0.83 is that the Douglas till was locally sheared to strains > ~20 over much of its thickness. Higher strains cannot be precluded or confirmed.

One question that arises from these results is why the Douglas till sampled from the field, in many cases, has larger S_1 values (up to 0.98) than the steady-state value (0.83) from ring-shear experiments. The explanation for this may reflect a difference in grain-size distribution between the field samples and ring-shear samples. The samples of Douglas till collected from the field for this study had a much lower sand content (10% versus 72%) and higher silt/clay content (90% versus 23%) than the samples of Douglas till used in ring-shear experiments (samples for ring-shear experiments were collected early in the project from an area along the lakeshore father to the northeast, where the till is coarser (Need, 1980)). This explanation agrees with the results of Thomason and Iverson (2006), who found in ring-shear experiments that stronger steady-state sand-particle fabrics developed in the Batestown till of the Lake Michigan lobe, which also had a lower sand (49% versus 72%) and higher silt/clay (34% versus 23%) content than the Douglas till used in the ring-shear experiments. Thomason and Iverson (2006) suggested that greater sand content and lower silt/clay content may impede alignment of sand-sized particles. Similarly, Hooyer et al. (in press) found that stronger AMS fabrics developed in the Batestown till in ring-shear experiments than in the Douglas till. These results indicate that tills containing more silt/clay and less sand develop stronger fabrics. Therefore, it is perhaps not surprising that stronger fabrics were measured in the field samples of the Douglas till, owing to its much higher silt/clay content and lower sand content.

D. Did the Douglas till deform uniformly over its full thickness?

A primary goal of this study was to determine if the Douglas till was transported in a thick, pervasively deforming subglacial layer (e.g. Alley 1986; Boulton and Hindmarsh, 1987). Two lines of evidence suggest the Douglas till was *not* deformed pervasively over its full thickness. The first is that S_1 values at certain depths are low relative to the steady-state, ring-shear value. S_1 values < 0.70 occur in all profiles except for BC2, BR3, and MR4, and S_1 values are as low as 0.54 in BC3. In fact, the only profile that does not have S_1 values < 0.83 is BR3 (Figures 3.3 and 3.4). This indicates that strain at some depths in the till was much smaller (<20) than that required by the bed-deformation model (>100). The second line of evidence is that azimuth changes significantly with depth in most profiles (Figure 3.11). If the Douglas till had been unidirectionally and pervasively deformed to high strains over its full thickness, we would expect to find relatively uniform fabric azimuths with depth, all with S_1 eigenvalues of at least 0.83.

Microshear orientations were measured in an attempt to establish a second criterion for determining if the Douglas till was sheared to high strains. However, microshears were not useful because their dip directions were not consistent with results of ring-shear experiments and thus could not be linked to strain magnitude. In these experiments, Riedel shears that dipped in the "down-glacier" direction were observed (Figure 1.2) (Thomason and Iverson, 2006), but microshears in this study dipped in the "up-glacier" direction (Figure 3.1), either to the northeast or northwest. There is not an obvious explanation for this difference between the field and experimental observations.

The microshears of this study, however, were observed only locally within thin sections and within a minority of the thin sections studied. The rarity of these microshears may indicate that their origin is different from the oppositely dipping Riedel shears that were ubiquitous in till sheared experimentally.

E. Origin of transverse fabrics

Another objective of this study was to illuminate the origin of transverse fabrics in the Douglas till. Ring-shear experiments demonstrate unequivocally that strongly clustered fabrics develop in the direction of shear at strains > ~20. 63% of the fabrics transverse to the regional flow direction measured in the Douglas till have $S_1 \geq 0.83$ and hence are strongly clustered. Therefore, given that there is no experimental evidence for transverse fabric development and strong evidence for clustering of experimental fabrics parallel to the shear direction, fabrics transverse to the regional ice-flow direction, as indicated by flutes nearby, are interpreted to be parallel to the local ice-flow direction. This interpretation implies major differences between the orientation of flutes and some local ice-flow directions and agrees with the northwest plunge of most transverse fabrics (Figures 3.9 and 3.10) because particles, regardless of size, gently plunged "up-glacier" in ring-shear experiments conducted to high strains (Hooyer et al., in press; Iverson et al., in press). Thus, if transverse fabrics formed parallel to the local flow direction, they should indeed plunge mostly to the northwest rather than to the southeast. These ring-shear results are supported by the generally up-glacier (northeast) plunges of particle fabrics that are parallel to the regional flow direction in this study (Figure 3.7 and 3.8).

F. Heterogeneous deformation of the bed

This interpretation of the transverse fabrics implies that flow direction varied substantially along the modern shoreline of Lake Superior over distances of a few meters to a few kilometers. One possible explanation for such variation could be that regional ice-flow direction was spatially variable, but because drastic changes in fabric direction occur over just a few meters, such as between BC3 and BC4 (Figure 3.5), this explanation is not satisfactory. An alternative hypothesis is that deformation of the bed occurred in an anastomosing pattern in plan view, such that deformable areas of the bed sheared around less deformable areas of the bed. This type of heterogeneous deformation would result in diverging and converging shear paths in the till, which would create variable fabric directions over short distances as seen in the Douglas till.

This explanation for the origin of transverse fabrics is consistent with the deforming-bed mosaic model envisioned by Piotrowski et al. (2004) (see also Piotrowski and Kraus, 1997; Larsen et al., 2004). This conceptual model hypothesizes the co-existence of deforming and stable patches of the bed that change size and shape with time and can also be created and destroyed with time. It implies that a given area of the bed will experience multiple phases of deformation and stability during a glacier occupation, such that any deformational signatures found in the bed, such as fabric and microshears, are interpreted as the result of cumulative, heterogeneous deformation over time.

This type of heterogeneous deformation can result from permeability variations in the bed because till strength depends on permeability. Since till behaves as a Coulomb

(frictional) plastic material (Iverson et al., 1998; Tulaczyk et al., 2000), its shear strength is described by the Coulomb-Terzaghi equation:

$$\tau = c + (p_i - p_w) \tan\phi,$$

where τ is total shear strength, c is the cohesion among particles, ϕ is the angle of internal friction among particles, p_i is the ice overburden pressure, and p_w is the pore-water pressure. Pore-water pressure acts to support some of the ice overburden pressure, so $p_i - p_w$ is the effective normal stress exerted by the ice. Till will deform when the shear stress applied by ice to the bed surface equals τ. The link between permeability and τ arises from the fact that pore-water pressure is controlled by permeability. Low-permeability tills drain water less readily, which means pore-water pressure must build in them to provide the hydraulic gradient necessary to push the supplied water discharge through the till. In accordance with the Coulomb-Terzaghi equation, pore-water pressure weakens till, causing it to be more susceptible to deformation. In contrast, high permeability tills can drain water more easily, inhibiting high pore-water pressure and associated deformation.

Hydraulic conductivity, which for pore water at a given temperature is a surrogate for permeability, can vary by 1-2 orders of magnitude in most geologic formations (Freeze and Cherry, 1979) and has been shown to vary by up to five orders of magnitude in tills due to lateral variations in silt/clay percentage and the degree of fracturing (Stephenson et al., 1988; Simpkins et al., 1990). Thus, till strength will also vary by 1-2 orders of magnitude or more because till strength depends linearly on pore-water pressure, which in turn depends linearly on permeability. Therefore, heterogeneous deformation of the bed is expected.

Furthermore, separation between the ice and bed by a thin layer of water can occur when elevated pore-water pressures are sustained (e.g. Iverson et al., 2003). In that case, clasts protruding from the base of the ice may plow through the bed and cause local deformation just beneath the glacier sole (Brown et al., 1987; Iverson, 1999; Iverson et al., 2007). If the water layer thickens, such that clasts at the bed surface no longer touch the glacier sole, bed deformation will halt (Iverson et al., 2003). Ice-bed decoupling would then cause shear stresses to become concentrated on surrounding areas of the bed where deformation would occur (Iverson et al., 1995; 1999; Fischer and Clarke, 2001). In the deforming-bed mosaic model, Piotrowski et al. (2004) favor this heterogeneous coupling of ice with the bed as the most likely mechanism for heterogeneous deformation of the bed.

Partitioning between bed deformation, plowing, and sliding, is controlled by the magnitude of basal water pressure and discharge (Iverson et al., 2003; 2007), which can vary significantly in time and space (across distances as small as a few meters). This variability is due not only to permeability variations of the bed but to seasonal, diurnal, and even hourly fluctuations in meltwater input to the bed (Iken and Bindschadler, 1986; Murray and Clarke, 1995; Iverson et al., 1995; Fischer and Clarke, 2001; Lappegard et al., 2006; Truffer and Harrison, 2006). Basal water pressure also depends on the geometry of the drainage system at the ice-bed interface (Iverson, 1999), which can evolve and change paths over time in response to seasonal changes in meltwater flux and rainwater input (e.g. Ensminger et al., 1999). This means that the location and the span of time in which ice-bed decoupling occurs can vary significantly, and as a result, the style of basal motion can be variable, both temporally and spatially. This variability has

recently been emphasized in several studies to explain field characteristics of basal sediments that are inconsistent with unidirectional, deep, pervasive deformation of the bed (e.g. Piotrowski and Kraus, 1997; Hoffmann and Piotrowski, 2001; Knight, 2002; Piotrowski et al., 2004; 2006).

G. Deposition and deformation of the Douglas till

Based on results of this study and the discussion outlined above, the following conceptual model is reasonable for the deposition and deformation of the Douglas till (Figure 4.1). Due to the Douglas till's high clay content and dearth of gravel-sized and larger particles, its protolith is believed to be lake sediment derived from a proglacial lake that developed during an earlier stage of the Superior lobe. The Superior lobe then readvanced over its own lake sediments, which were entrained, transported in ice, and re-deposited. Deposition most likely occurred by progressive accretion due to lodgement with concurrent deformation of the bed that occurred heterogeneously in either decimeter-thick zones or in a somewhat thinner zone just beneath the glacier sole near plowing particles (Figure 4.1). Fabric azimuth variations with depth rule out deep deformation of the bed at any one time. Lateral heterogeneity in deformation was most likely the result of permeability variations in the bed or heterogeneous decoupling of ice from the bed, which resulted in anastomosing zones of deformation over the bed area. As a result, converging and diverging shear paths in the till created variable fabric directions over lateral distances as small as a few meters (Figure 4.1). As the bed accreted through lodgement, zones of deformation moved upward with time, resulting in variable fabric strengths and directions with depth. Variations in subglacial water pressure due to

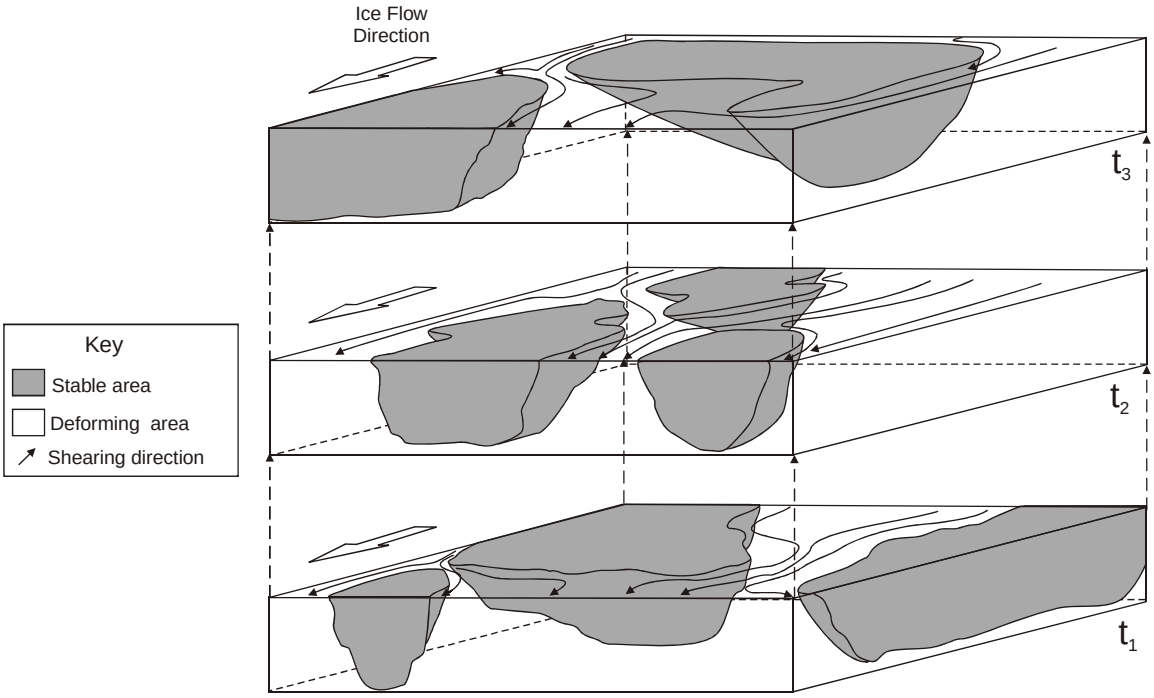

Figure 4.1. Schematic depiction of spatially heterogeneous deformation occurring in the Douglas till as it is progressively accreted to the bed in layers deforming near the glacier sole at three different times, denoted $t_{1\text{-}3}$. The resultant till unit is a composite of these superimposed layers.

seasonal fluctuations in meltwater supplied to the bed may have caused this process to be temporally variable, such that a given area of the bed experienced multiple phases of deformation and stability.

This conceptual model differs from the simpler bed-deformation model that has usually been advocated (e.g., Alley et al., 1986; Boulton and Hindmarsh, 1987; Jenson et al., 1995), which involves pervasive simple shear of the bed over all or most of its thickness at any one time. This difference is important because in the simpler model basal sediment transport is primarily by bed deformation, with the till layer sustained primarily by erosion of substrate below the deforming bed (e.g., Alley et al., 1987). In

contrast, the model of an accreting, heterogeneously deforming bed requires transport of sediment in ice, followed by lodgement deposition and associated bed deformation near the glacier sole. Thus, sediment transport includes but is not dominated by shear deformation of the bed.

Nevertheless, the fabric data collected in this study do not rule out the possibility of till being sheared locally at depth to the high strains required by the bed-deformation model. Pervasive deformation well below the glacier sole may have occurred in some parts of the bed. For example, a few sequences in the Douglas till data have strong fabrics with uniform or nearly uniform azimuths with depth, which suggest pervasive deformation may have taken place. These sequences include BC4 from 13.2 m to 14.6 m and all of BR3 (Figures 3.3-3.6). However, because till develops a steady-state fabric strength at moderately low strains, we cannot necessarily conclude that the till in these zones was subjected to the high strains required by the bed-deformation model. Moreover, locally strong fabrics may have developed time-transgressively as the till unit accreted by lodgement, with deformation at any one time occurring only near the glacier sole (Larsen et al., 2004).

H. Implications for glacier advance and climate change

Clark (1994) suggested that readvances of lobes of the Laurentide ice sheet margin during times of rapidly warming climate was a result of flow instability associated with deforming-bed conditions. The fabric data of this study do not rule out this possibility for the Superior lobe. The readvance of the Superior lobe that was responsible for depositing the Douglas till occurred during a time of rapidly warming

climate around 11,000 calendar years ago (Clayton, 1984), after the Younger Dryas cold period (13, 000 to 11,400 calendar years ago) (Clark et al., 2001). Warming may trigger flow instability by increasing meltwater production, thereby increasing water discharge to the bed and basal water pressure. This increase in basal water pressure may trigger deformation of the bed and glacier advance. This is important because such advances may have played a critical role in the routing of meltwater to the North Atlantic and the resultant modulation of its thermohaline circulation (Clark, 1994; Clark et al., 2001). Although the data of this study seem to indicate the deformation of the bed was heterogeneous and shallow as the bed accreted, deformation may have, nevertheless, affected a sufficient fraction of the glacier sole to accelerate glacier flow and cause advance, despite the warming climate.

CHAPTER 5. CONCLUSIONS

Results from this study support Johnson's (1980; 1983) conclusion that the Douglas member is till and not lake sediment. Strong, unimodal AMS fabrics and microshears in the Douglas member indicate that it was sheared during deformation of the bed (Thomason and Iverson, 2006; Hooyer et al., in press). In contrast, if the Douglas member was lake sediment unmodified by shear, girdle fabrics would be expected. Due to the Douglas member's fine-grained texture, lack of gravel-sized and larger particles, and proximity to shoreline deposits (Johnson, 1983), its protolith is interpreted to be lake sediment derived from a proglacial lake of the Superior lobe.

Consistent with previous studies, azimuths from AMS and sand-particle fabrics are similar but not identical (e.g., Thomason, 2006). The difference in azimuths is likely the result of error and noise associated with measurement of sand-particle orientations. Nevertheless, results from this study provide further support for use of AMS as an indicator of particle fabric and ultimately of strain magnitude and direction.

AMS fabrics in the Douglas till are, in general, sufficiently strong that the high strains required by the bed-deformation model cannot to be ruled out (Hooyer et al., in press; Iverson et al., in press). Approximately 63% of S_1 eigenvalues are greater than or equal to the steady state value (0.83) attained in ring-shear experiments using the Douglas till. However, AMS fabric strengths and directions are variable both laterally, over distances of a few meters, and with depth, over distances of a few decimeters, which suggests the Douglas till was not deformed to high strains (>100) uniformly over its

entire thickness as implied by the bed-deformation model. Instead, the till was likely transported englacially and deposited by progressive accretion due lodgment with concurrent deformation of the bed occurring in either decimeter thick zones or in thinner zones just beneath the glacier sole near plowing particles. Deformation was probably both spatially and temporally heterogeneous due to variations in permeability and subglacial water pressure at the bed. As the bed progressively accreted, zones of deformation moved upwards with time, resulting in variable fabric strengths and directions with depth.

Approximately 63% of AMS fabrics in the Douglas till that are oriented transverse to the regional glacier-flow direction, as indicated by flutes nearby, are strongly clustered with S_1 eigenvalues ≥ 0.83. These fabrics are interpreted to be parallel to the local ice-flow direction because ring-shear experiments demonstrate that strongly clustered AMS fabrics develop parallel to the shear direction. Transverse fabrics are interpreted to have resulted from heterogeneous deformation of the bed, which created converging and diverging shear paths in the till. This interpretation provides an explanation for the variability in fabric direction that occurs over distances of only a few meters and agrees with the observation that fabrics oriented transverse to the regional ice-flow direction plunge preferentially to the northwest; results of ring-shear experiments indeed indicate the AMS fabrics plunge up-glacier.

This study supports the hypothesis that a glacier typically moves by some combination of deformation, plowing, and sliding (Fischer and Clarke, 2001; Piotrowski et al., 2004; Larsen et al., 2004), rather than by uniform, deep, simple shear of the bed,

which is commonly advocated (e.g., Alley et al., 1986; Boulton and Hindmarsh, 1987; Jenson et al., 1995). This study also demonstrates the benefit of using experiments to interpret the deformational history of till (Thomason and Iverson, 2006; Thomason, 2006; Hooyer et al., in press; Iverson et al., in press).

APPENDEX

Table A1. AMS Profiles

Bardon Creek, BC2										
		V_1		V_2		V_3				
Bench	n	azi,°	pl,°	azi,°	pl,°	azi,°	pl,°	S_1	S_2	S_3
BC2-16.8	25	167	11	263	25	56	62	0.82	0.16	0.02
BC2-16.6	25	126	14	33	10	268	72	0.93	0.05	0.02
BC2-16.4	25	144	1	237	66	54	24	0.97	0.02	0.01
BC2-16.2	25	329	21	69	24	203	58	0.98	0.02	0.00
BC2-16.0	24	333	15	67	15	200	69	0.96	0.03	0.01
BC2-15.8	25	330	3	239	6	87	83	0.91	0.08	0.01
BC2-15.6	25	300	9	38	43	201	46	0.94	0.05	0.01
BC2-15.4	25	274	26	14	20	137	56	0.82	0.15	0.03
BC2-15.2	25	303	9	212	9	76	77	0.72	0.24	0.04
BC2-15.0	25	332	18	241	5	134	71	0.89	0.09	0.02
BC2-14.8	25	122	1	212	21	30	69	0.88	0.06	0.06
BC2-14.6	25	135	10	44	7	279	77	0.85	0.13	0.02
BC2-14.4	25	126	5	35	13	234	76	0.78	0.20	0.02
BC2-14.2	25	316	1	226	6	53	84	0.86	0.12	0.02
BC2-14.0	25	188	12	93	19	307	67	0.78	0.19	0.03
BC2-13.8	25	117	21	210	8	320	68	0.83	0.12	0.05
BC2-13.6	25	98	25	311	60	194	14	0.73	0.16	0.11
BC2-13.4	25	149	2	58	44	241	46	0.79	0.19	0.02
BC2-13.2	25	341	7	251	4	131	82	0.83	0.12	0.05
BC2-13.0	25	340	2	71	40	248	50	0.91	0.07	0.02
BC2-12.8	25	339	17	113	66	244	16	0.84	0.12	0.04
BC2-12.6	25	342	8	248	30	86	58	0.88	0.08	0.04
BC2-12.4	25	329	6	59	7	198	80	0.91	0.05	0.04
BC2-12.2	25	303	7	208	36	43	53	0.87	0.10	0.03
BC2-12.0	25	169	7	261	20	62	69	0.72	0.26	0.02
BC2-11.8	25	346	9	88	55	250	34	0.88	0.08	0.04
BC2-11.6	25	324	9	64	49	226	39	0.72	0.22	0.06

Table A1. (continued)

Bardon Creek, BC3										
		V_1		V_2		V_3				
Bench	n	azi,°	pl,°	azi,°	pl,°	azi,°	pl,°	S_1	S_2	S_3
BC3-16.6	25	197	42	44	45	300	14	0.83	0.14	0.03
BC3-16.4	25	340	32	110	46	232	27	0.77	0.21	0.02
BC3-16.2	25	130	11	27	48	229	40	0.71	0.27	0.02
BC3-16.0	25	112	1	21	52	203	38	0.88	0.11	0.01
BC3-15.8	25	129	4	38	9	243	80	0.89	0.09	0.02
BC3-15.6	25	114	8	6	65	207	24	0.72	0.18	0.10
BC3-15.4	25	111	9	4	62	205	27	0.79	0.17	0.04
BC3-15.2	25	131	2	37	60	222	30	0.79	0.18	0.03
BC3-15.0	25	279	2	189	2	45	87	0.87	0.11	0.02
BC3-14.8	25	126	24	234	36	10	45	0.96	0.03	0.01
BC3-14.6	25	138	17	229	5	334	73	0.85	0.14	0.01
BC3-14.4	25	273	15	161	55	12	31	0.74	0.20	0.06
BC3-14.2	25	126	35	286	53	30	10	0.90	0.09	0.01
BC3-14.0	25	268	47	146	25	39	31	0.64	0.31	0.05
BC3-13.8	25	297	51	98	38	195	9	0.77	0.20	0.03
BC3-13.6	25	299	17	36	21	173	62	0.91	0.08	0.01
BC3-13.4	25	300	7	200	52	35	37	0.93	0.04	0.03
BC3-13.2	25	330	17	66	16	196	66	0.93	0.06	0.01
BC3-13.0	25	349	34	94	22	211	48	0.74	0.24	0.02
BC3-12.8	25	346	24	77	2	170	66	0.91	0.07	0.02
BC3-12.6	25	9	26	278	2	184	64	0.85	0.14	0.01
BC3-12.4	25	319	15	60	36	210	50	0.82	0.14	0.04
BC3-12.2	25	334	26	70	11	181	61	0.54	0.43	0.03
BC3-12.0	25	2	24	94	5	194	65	0.79	0.17	0.04
BC3-11.8	25	334	27	70	12	181	60	0.85	0.13	0.02
BC3-11.6	25	342	33	115	46	235	25	0.91	0.06	0.03

Table A1. (continued)

Bardon Creek, BC4										
		V_1		V_2		V_3				
Bench	n	azi,°	pl,°	azi,°	pl,°	azi,°	pl,°	S_1	S_2	S_3
BC4-15.4	25	339	17	240	28	97	56	0.95	0.04	0.01
BC4-15.2	25	40	41	132	3	226	48	0.69	0.30	0.01
BC4-15.0	25	217	3	127	0	30	87	0.78	0.18	0.04
BC4-14.8	25	29	21	292	15	169	63	0.89	0.08	0.03
BC4-14.6	25	52	21	308	32	169	50	0.95	0.04	0.01
BC4-14.4	25	42	31	171	46	293	28	0.97	0.02	0.01
BC4-14.2	25	41	31	293	29	169	46	0.93	0.05	0.02
BC4-14.0	25	45	27	310	10	202	61	0.97	0.02	0.01
BC4-13.8	25	58	22	323	12	206	65	0.93	0.06	0.01
BC4-13.6	25	66	19	327	25	189	57	0.94	0.04	0.02
BC4-13.4	25	77	25	333	27	204	51	0.93	0.05	0.02
BC4-13.2	25	69	23	327	25	196	55	0.93	0.06	0.01
BC4-13.0	25	83	28	350	6	250	61	0.85	0.14	0.01
BC4-12.8	25	81	4	348	36	176	54	0.58	0.40	0.02
BC4-12.6	25	355	26	98	24	224	53	0.82	0.16	0.02
BC4-12.4	25	354	20	98	33	239	50	0.85	0.13	0.02
BC4-12.2	25	319	24	53	9	162	65	0.87	0.12	0.01
BC4-12.0	25	238	3	328	19	140	70	0.66	0.32	0.02
BC4-11.8	25	346	35	94	24	212	45	0.64	0.32	0.04
BC4-11.6	25	338	19	79	30	220	53	0.89	0.07	0.04

Table A1. (continued)

Bardon Creek, BC5										
		V_1		V_2		V_3				
Bench	n	azi,°	pl,°	azi,°	pl,°	azi,°	pl,°	S_1	S_2	S_3
BC5-14.0	25	107	15	342	65	202	20	0.94	0.05	0.01
BC5-13.8	25	162	0	72	60	252	30	0.79	0.14	0.07
BC5-13.6	25	142	22	255	44	34	37	0.85	0.09	0.06
BC5-13.4	25	140	10	17	73	233	14	0.87	0.09	0.04
BC5-13.2	25	152	11	49	48	251	40	0.64	0.31	0.05
BC5-13.0	25	39	37	135	9	237	51	0.88	0.09	0.03
BC5-12.8	25	90	34	355	7	255	55	0.67	0.28	0.05
BC5-12.6	25	35	45	299	6	203	44	0.78	0.19	0.03
BC5-12.4	25	355	28	108	36	237	41	0.88	0.09	0.03
BC5-12.2	25	9	24	112	26	243	53	0.80	0.18	0.02
BC5-12.0	25	71	33	326	22	208	49	0.74	0.24	0.02
BC5-11.8	25	317	32	65	27	186	46	0.88	0.09	0.03
BC5-11.6	25	299	5	30	13	186	76	0.79	0.14	0.07
BC5-11.4	25	111	31	354	37	229	38	0.80	0.14	0.06
BC5-11.2	25	29	56	283	11	186	32	0.73	0.25	0.02
BC5-11.0	25	96	15	330	65	191	19	0.64	0.33	0.03
BC5-10.8	25	62	17	331	3	232	73	0.74	0.22	0.04
BC5-10.6	25	117	20	25	5	281	70	0.93	0.05	0.02
BC5-10.4	25	10	30	110	17	226	54	0.64	0.34	0.02
BC5-10.2	25	63	28	329	8	225	61	0.73	0.23	0.04
BC5-10.0	25	53	6	318	40	150	49	0.58	0.37	0.05
BC5-9.8	25	285	20	194	2	100	70	0.69	0.22	0.09
BC5-9.6	25	132	1	40	61	223	29	0.88	0.09	0.03
BC5-9.4	25	289	9	20	6	146	79	0.89	0.09	0.02
BC5-9.2	25	142	8	260	74	50	14	0.93	0.05	0.02
BC5-9.0	25	300	11	190	62	35	26	0.70	0.26	0.04

Table A1. (continued)

Brule River, BR2										
		V_1		V_2		V_3				
Bench	n	azi,°	pl,°	azi,°	pl,°	azi,°	pl,°	S_1	S_2	S_3
BR2-5.0	25	120	37	24	8	283	52	0.70	0.27	0.03
BR2-4.8	25	74	46	337	7	240	43	0.83	0.13	0.04
BR2-4.6	25	113	35	8	20	254	48	0.89	0.09	0.02
BR2-4.4	25	353	12	102	56	255	31	0.68	0.25	0.07
BR2-4.2	25	26	30	137	33	263	43	0.75	0.20	0.05
BR2-4.0	25	30	41	143	24	254	39	0.93	0.06	0.01
BR2-3.8	25	28	46	147	26	255	33	0.97	0.02	0.01
BR2-3.6	25	7	40	144	41	256	23	0.92	0.07	0.01
BR2-3.4	25	37	47	202	42	299	8	0.96	0.03	0.01
BR2-3.2	25	31	70	196	19	288	5	0.82	0.15	0.03

Brule River, BR3										
		V_1		V_2		V_3				
Bench	n	azi,°	pl,°	azi,°	pl,°	azi,°	pl,°	S_1	S_2	S_3
BR3-5.0	25	1	18	97	18	230	64	0.86	0.12	0.02
BR3-4.8	25	21	31	242	52	123	21	0.96	0.03	0.01
BR3-4.6	25	32	30	142	31	267	44	0.98	0.01	0.01
BR3-4.4	25	31	19	300	3	201	71	0.97	0.03	0.00
BR3-4.2	25	29	20	294	15	169	65	0.98	0.02	0.00
BR3-4.0	25	30	27	126	13	240	60	0.94	0.05	0.01
BR3-3.8	25	30	28	282	31	154	46	0.91	0.05	0.04
BR3-3.6	25	26	40	261	35	146	31	0.88	0.09	0.03
BR3-3.4	25	29	31	201	59	297	3	0.89	0.06	0.05
BR3-3.2	25	30	31	141	31	266	44	0.95	0.03	0.02

Table A1. (continued)

Middle River, MR3										
		V_1		V_2		V_3				
Bench	n	azi,°	pl,°	azi,°	pl,°	azi,°	pl,°	S_1	S_2	S_3
MR3-17.0	25	331	7	240	11	93	77	0.83	0.16	0.01
MR3-16.8	25	353	10	252	48	92	40	0.96	0.03	0.01
MR3-16.6	25	2	9	268	19	116	69	0.80	0.17	0.03
MR3-16.4	25	355	8	260	32	99	57	0.85	0.13	0.02
MR3-16.2	25	358	14	88	0	179	76	0.91	0.08	0.01
MR3-16.0	25	9	12	277	8	153	76	0.63	0.36	0.01
MR3-15.8	25	7	9	277	1	180	81	0.85	0.14	0.01
MR3-15.6	25	354	9	264	1	167	81	0.90	0.09	0.01
MR3-15.4	25	342	11	248	18	102	68	0.82	0.17	0.01
MR3-15.2	25	338	17	71	12	194	69	0.67	0.30	0.03
MR3-15.0	25	331	20	66	14	189	66	0.93	0.06	0.01
MR3-14.8	25	324	15	58	14	190	69	0.94	0.05	0.01
MR3-14.6	25	327	23	57	1	150	67	0.90	0.09	0.01
MR3-14.4	25	348	29	249	16	134	56	0.92	0.07	0.01
MR3-14.2	25	343	36	84	14	192	50	0.95	0.03	0.02
MR3-14.0	25	334	37	242	2	150	53	0.95	0.04	0.01
MR3-13.8	25	305	15	215	1	120	75	0.97	0.02	0.01
MR3-13.6	25	342	19	251	2	155	71	0.76	0.21	0.03
MR3-13.4	25	33	21	126	9	237	67	0.93	0.06	0.01
MR3-13.2	25	35	20	302	7	194	69	0.97	0.02	0.01

Middle River, MR4										
		V_1		V_2		V_3				
Bench	n	azi,°	pl,°	azi,°	pl,°	azi,°	pl,°	S_1	S_2	S_3
MR4-16.0	25	3	41	265	9	166	48	0.94	0.04	0.02
MR4-15.8	25	20	41	277	14	172	45	0.77	0.21	0.02
MR4-15.6	25	243	1	334	46	151	44	0.76	0.21	0.03
MR4-15.4	25	261	26	359	16	118	58	0.89	0.08	0.03
MR4-15.2	25	251	26	345	9	93	62	0.83	0.16	0.01
MR4-15.0	25	230	16	329	28	114	57	0.96	0.03	0.01
MR4-14.8	25	208	7	299	9	81	78	0.90	0.08	0.02
MR4-14.6	25	4	0	274	8	96	82	0.95	0.04	0.01
MR4-14.4	25	14	7	275	51	109	38	0.96	0.03	0.01
MR4-14.2	25	12	0	282	23	103	67	0.96	0.03	0.01
MR4-14.0	25	216	6	309	25	114	64	0.97	0.03	0.00

Table A2. Sand Particle Fabric Profiles

Bardon Creek, BC2								
	Horizonal Plane				Vertical Plane			
Bench	n	m*	V_1, azimuth,^{o}	S_1	n	m*	V_1, azimuth,^{o}	S_1
BC2-16.8	131	15	18	0.71	91	20	42	0.62
BC2-16.6	101	14	129	0.67	94	25	126	0.71
BC2-16.4	84	10	132	0.62	124	24	85	0.55
BC2-16.2	97	10	320	0.66	119	25	75	0.67
BC2-16.0	89	7	134	0.54	71	13	111	0.66
BC2-15.8	139	12	327	0.54	81	17	73	0.65
BC2-15.6	96	7	16	0.52	117	22	325	0.58
BC2-15.4	105	7	36	0.55	80	12	104	0.59
BC2-15.2	100	10	349	0.58	66	13	127	0.70
BC2-15.0	81	8	25	0.59	99	17	126	0.60
BC2-14.8	106	9	110	0.60	68	10	116	0.58
BC2-14.6	125	11	335	0.59	85	20	105	0.64
BC2-14.4	66	5	131	0.55	98	19	131	0.56
BC2-14.2	87	9	132	0.57	83	16	99	0.67
BC2-14.0	65	6	334	0.54	72	13	107	0.68
BC2-13.8	68	6	58	0.57	91	20	135	0.68
BC2-13.6	131	11	120	0.61	80	14	132	0.61
BC2-13.4	70	7	119	0.55	91	15	88	0.59
BC2-13.2	90	7	133	0.58	76	11	71	0.61
BC2-13.0	95	9	316	0.59	103	16	56	0.56
BC2-12.8	98	11	317	0.71	83	13	100	0.58
BC2-12.6	113	10	11	0.54	68	11	20	0.55
BC2-12.4	75	9	320	0.63	112	16	325	0.54
BC2-12.2	117	10	90	0.54	102	22	124	0.63
BC2-12.0	138	9	32	0.51	96	16	85	0.57
BC2-11.8	105	11	7	0.64	93	17	44	0.57
BC2-11.6	95	10	22	0.63	102	27	318	0.69

* m is the number of particles in the major mode of rose diagrams

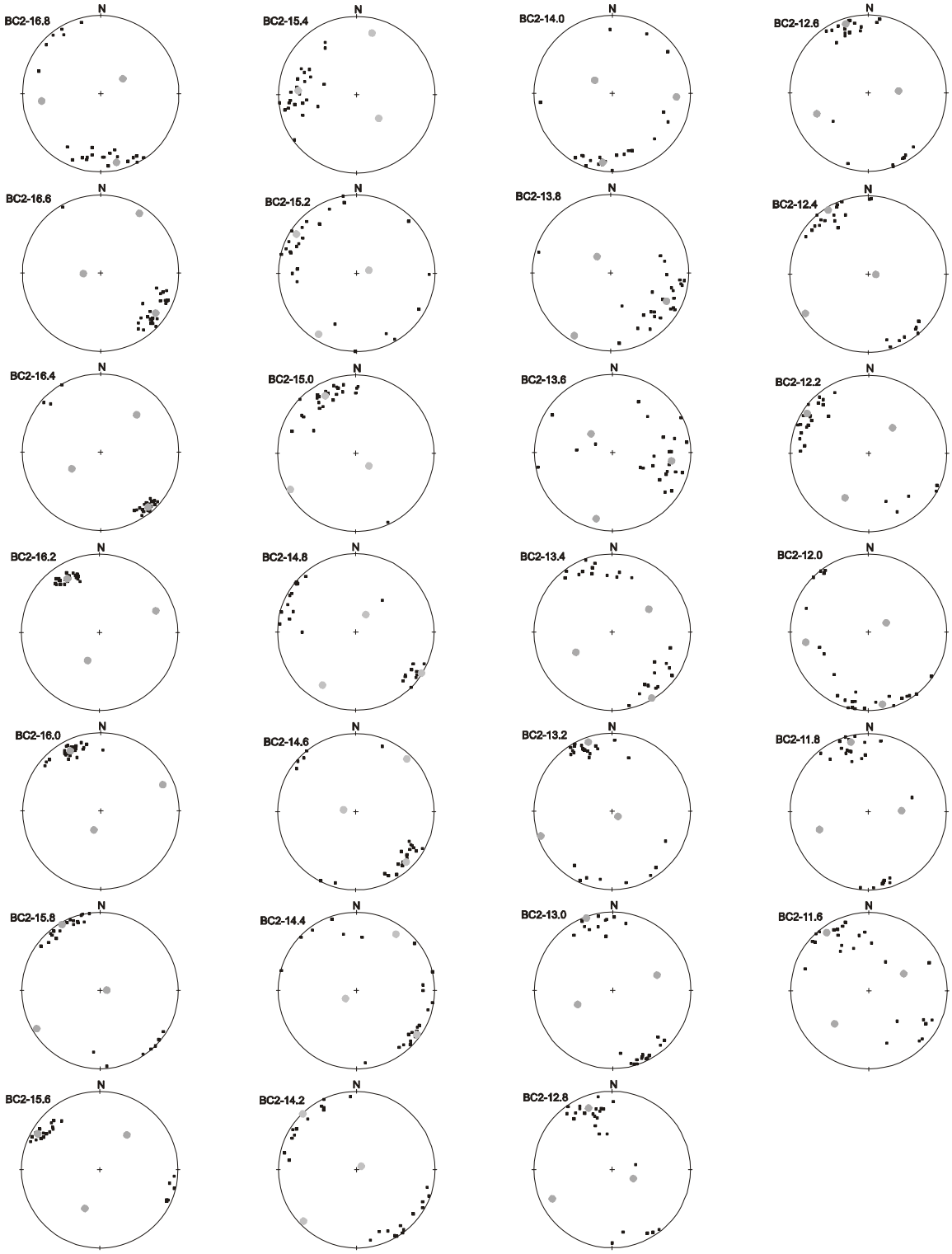

Figure A1. Stereoplots with directions of maximum magnetic susceptibility (k_1) from profile BC2 at Bardon Creek. BC2-# indicates the elevation above lake level (m). Grey dots are eigenvectors.

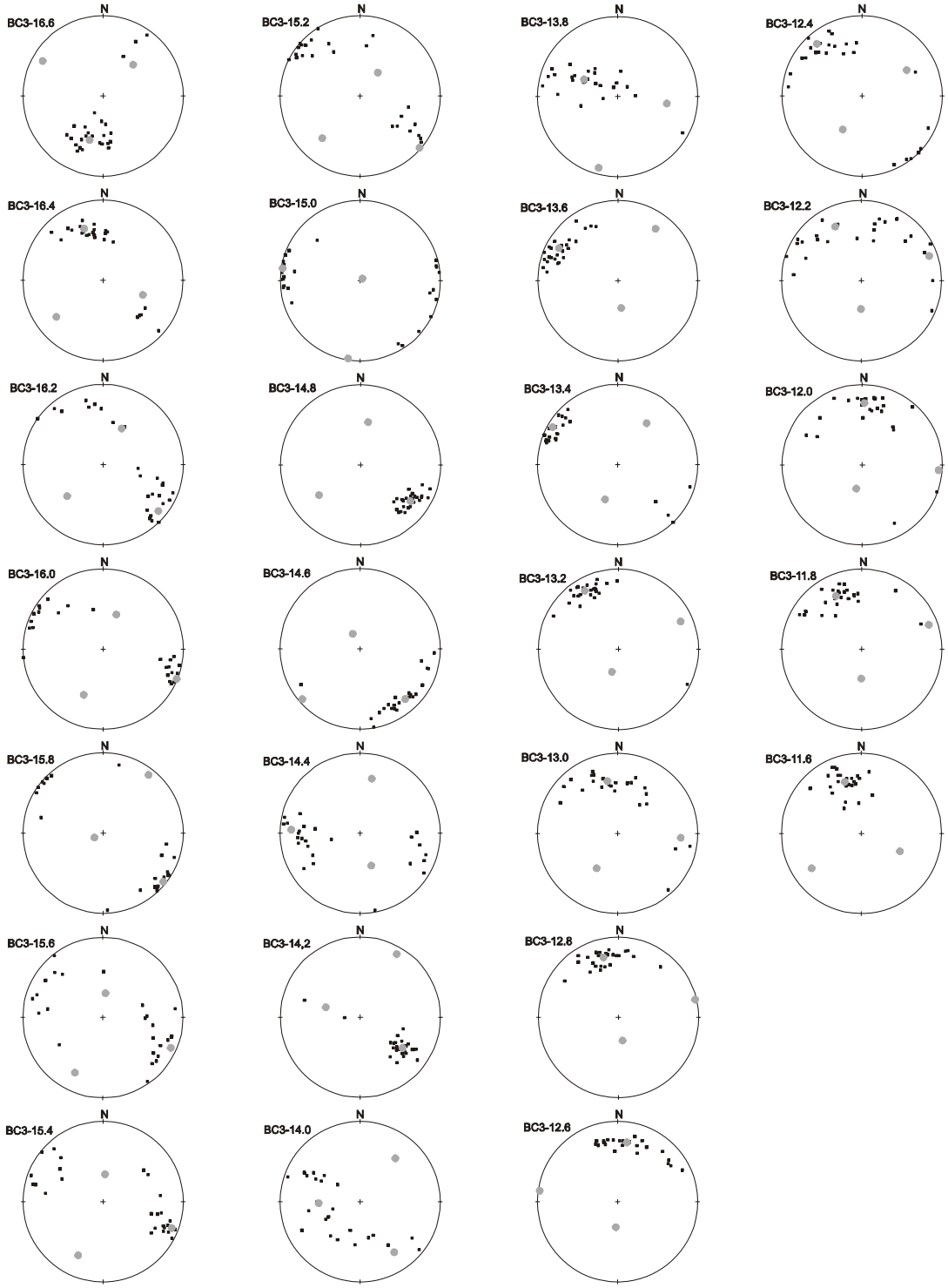

Figure A2. Stereoplots with directions of maximum magnetic susceptibility (k_1) from profile BC3 at Bardon Creek. BC3-# indicates the elevation above lake level (m). Grey dots are eigenvectors.

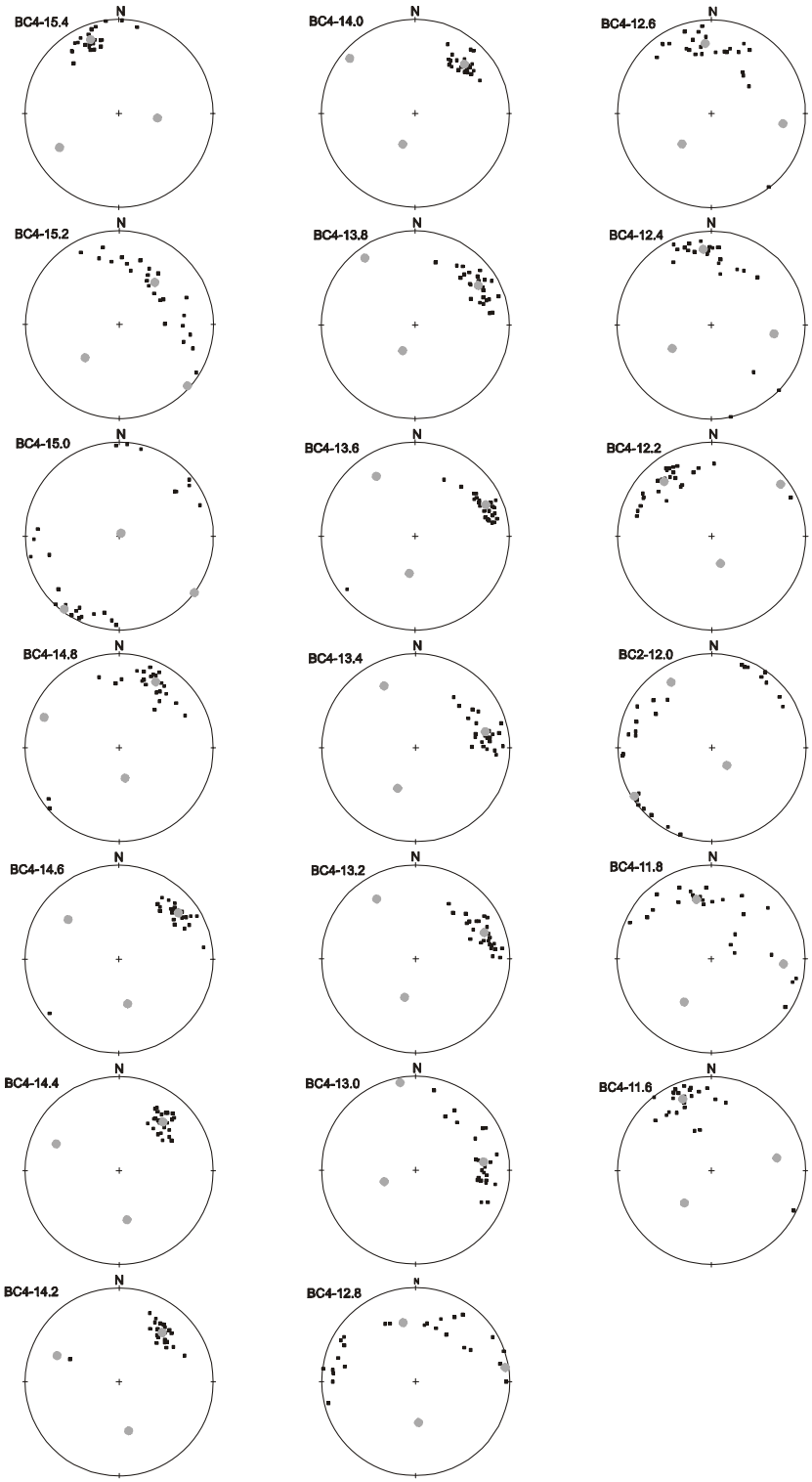

Figure A3. Stereoplots with directions of maximum magnetic susceptibility (k_1) from profile BC4 at Bardon Creek. BC4-# indicates the elevation above lake level (m). Grey dots are eigenvectors.

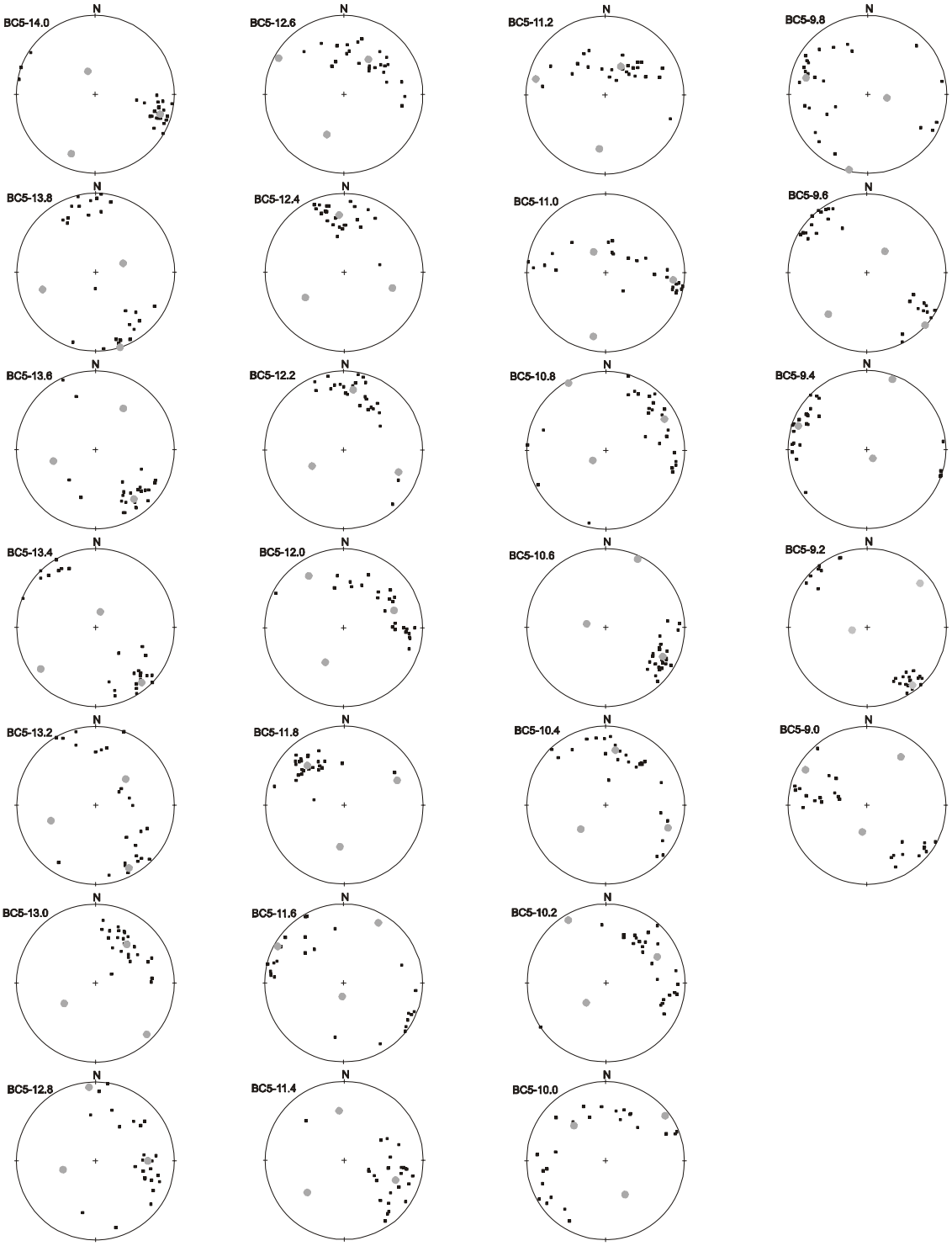

Figure A4. Stereoplots with directions of maximum magnetic susceptibility (k_1) from profile BC5 at Bardon Creek. BC5-# indicates the elevation above lake level (m). Grey dots are eigenvectors.

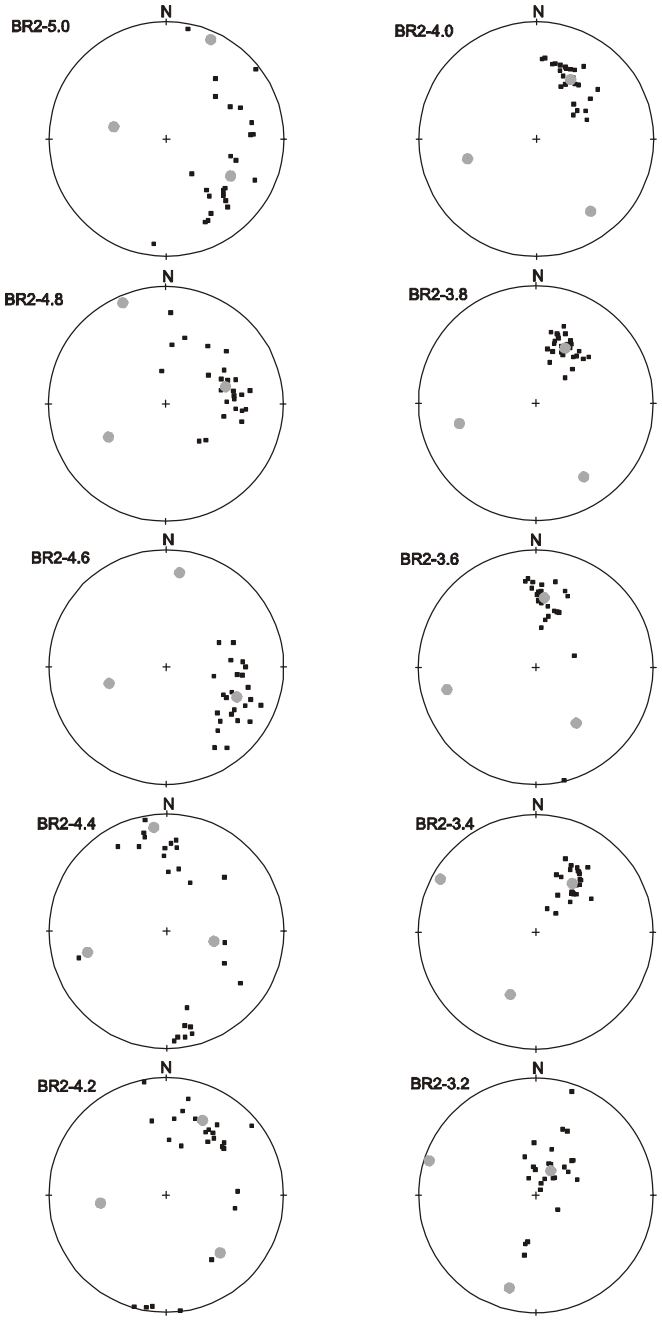

Figure A5. Stereoplots with directions of maximum magnetic susceptibility (k_1) from profile BR2 at Brule River. BR2-# indicates the elevation above lake level (m). Grey dots are eigenvectors.

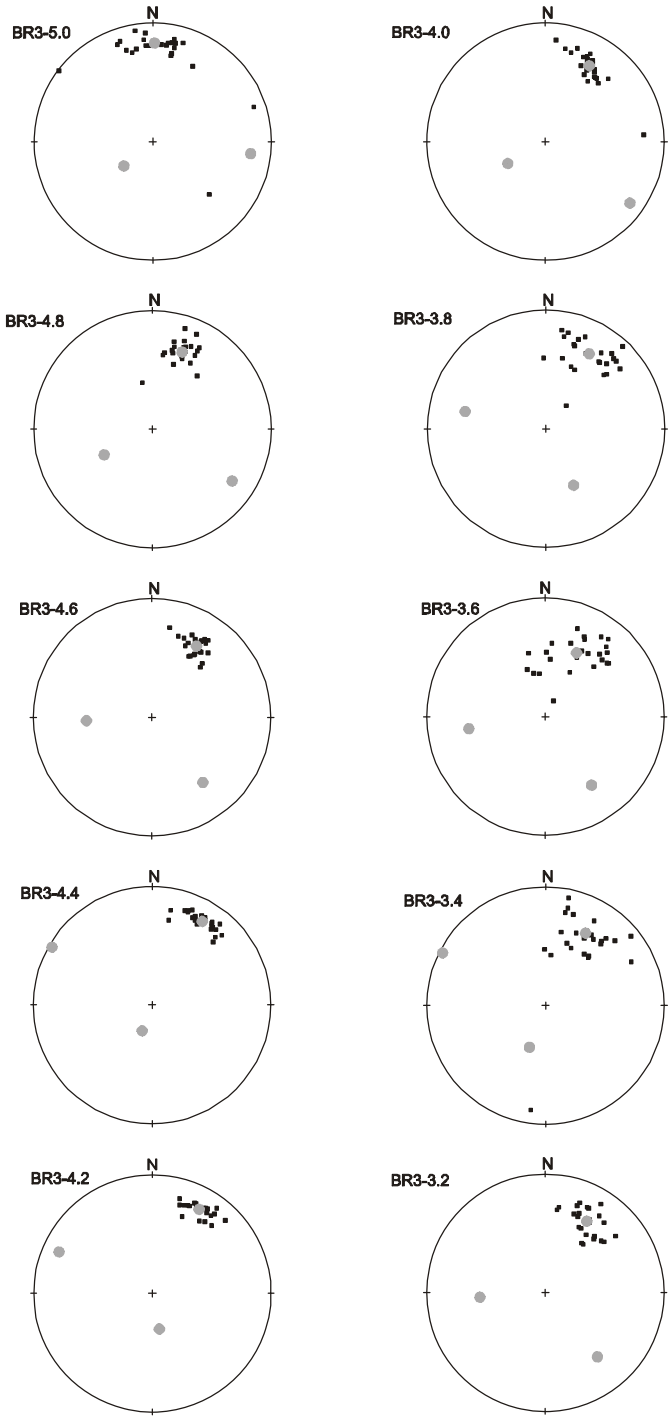

Figure A6. Stereoplots with directions of maximum magnetic susceptibility (k_1) from profile BR3 at Brule River. BR3-# indicates the elevation above lake level (m). Grey dots are eigenvectors.

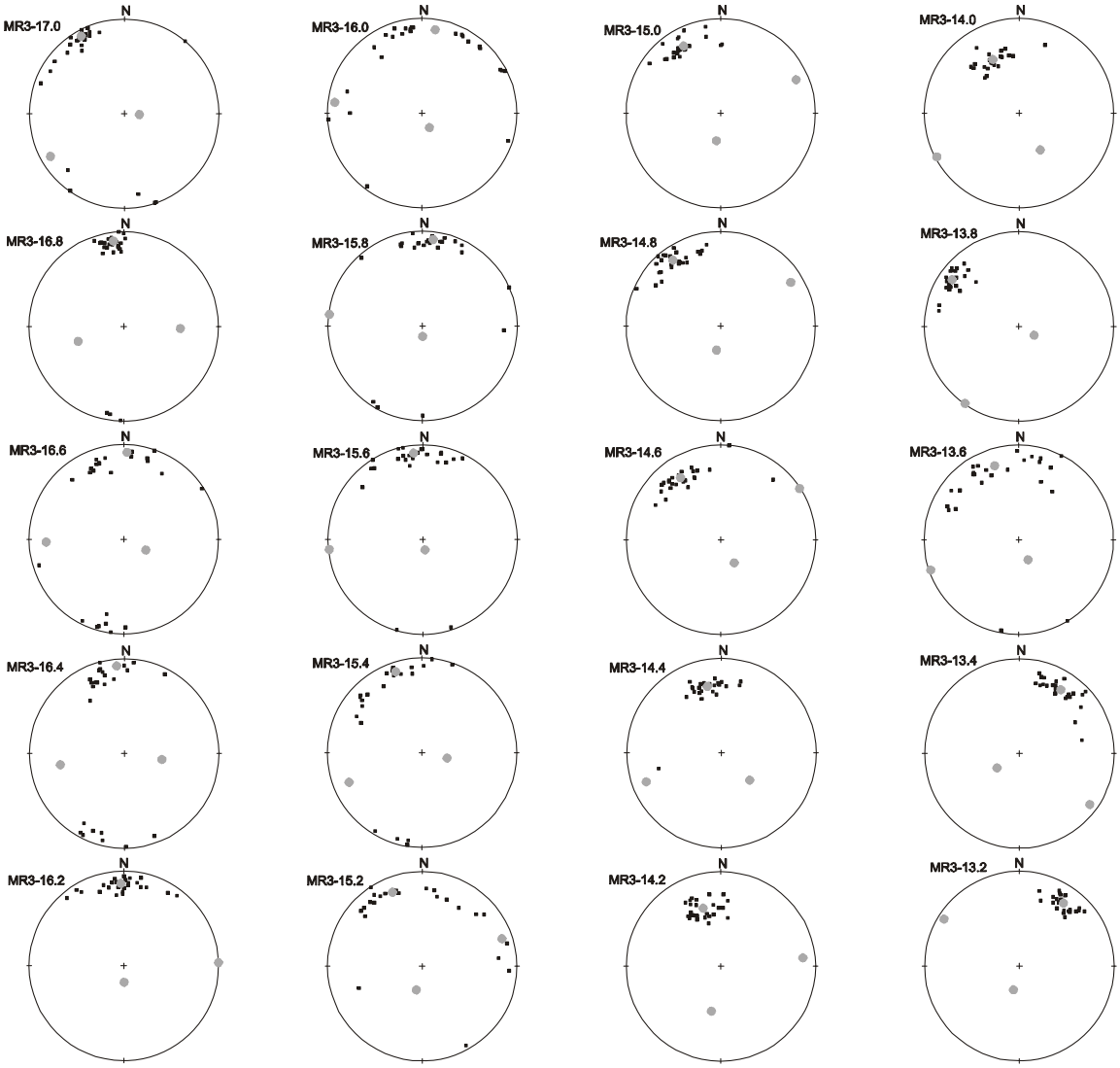

Figure A7. Stereoplots with directions of maximum magnetic susceptibility (k_1) from profile MR3 at Middle River. MR3-# indicates the elevation above lake level (m). Grey dots are eigenvectors.

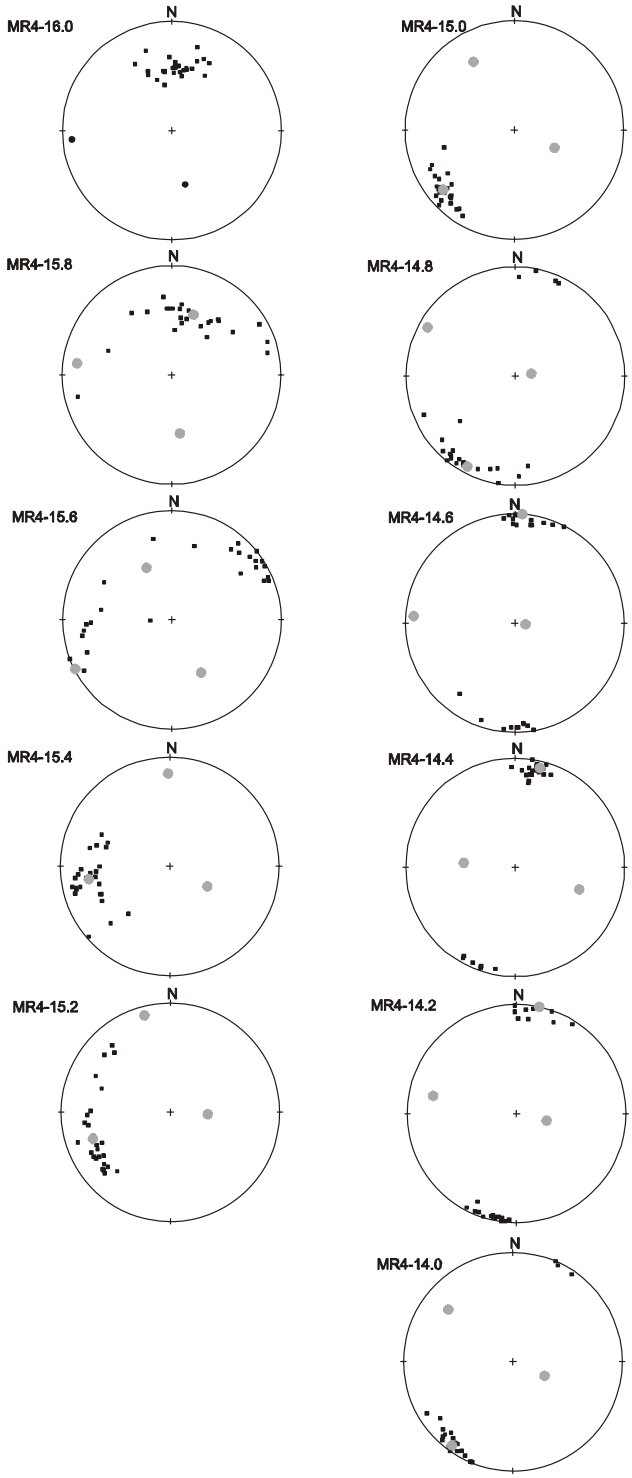

Figure A8. Stereoplots with directions of maximum magnetic susceptibility (k_1) from profile MR4 at Middle River. MR4-# indicates the elevation above lake level (m). Grey dots are eigenvectors.

REFERENCE LIST

Alley, R.B. 1991. Deforming-bed origin for southern Laurentide till sheets? *J. Glaciol.,* **37**(125), 67-76.

Alley, R.B., D.D. Blankenship, C.R. Bentley and S.T. Rooney. 1986. Deformation of till beneath ice stream B, West Antarctica. *Nature,* **322**(6074), 57-59.

Alley, R.B., D.D. Blankenship, C.R. Bentley and S.T. Rooney. 1987. Till beneath Ice Stream B. 3. Till Deformation: Evidence and Implications. *J. Geophys. Res.,* **92**(B9), 8921 - 8929.

Benn, D.I. 1995. Fabric signature of till deformation, Breidamerkurjökull, Iceland. *Sedimentology,* **42**(5), 735-747.

Benn, D.I. and T.J. Ringrose. 2001. Random variation of fabric eigenvalues: implications for the use of a-axis fabric data to differentiate till facies. *Earth Surf. Proc. Land.,* **26**(3), 295-306.

Bennett, M.R., R.I. Waller, N.F. Glasser, M.J. Hambrey and D. Huddart. 1999. Glacigenic clast fabrics: genetic fingerprint or wishful thinking? *J. Quat. Sci.,* **14**(2), 125-135.

Boulton, G.S. 1971. Till genesis and fabric in Svalbard, Spitsbergen. *In* Goldthwait, R.P., *ed. Till, a symposium.* Ohio State University Press, Columbus, Ohio, 41-72.

Boulton, G.S. 1987. A theory of drumlin formation by subglacial sediment deformation. *In* Menzies, J. and J. Rose, eds. *Drumlin Syposium.* Rotterdam, A.A. Balkema, 25-80.

Boulton, G.S. 1996. The theory of glacial erosion, transport and deposition as consequence of subglacial sediment deformation. *J. Glaciol.,* **42**(140), 43-62.

Boulton, G.S. and R.C.A. Hindmarsh. 1987. Sediment deformation beneath glaciers: rheology and geological consequences. *J. Geophys. Res.,* **92**(B9), 9059-9082.

Boulton, G.S., K.E. Dobbie and S. Zatsepin. 2001. Sediment deformation beneath glaciers and its coupling to the subglacial hydraulic system. *Quatern. Int.,* **86**(1), 3-28.

Brown, N.E., B. Hallet, and D.B. Booth. 1987. Rapid soft bed sliding of the Puget Sound glacial lobe. *J. Geophys. Res.,* **92**(B9), 8985 - 8997.

Carr, S.J. and J. Rose. 2003. Till fabric patterns and significance: particle response to subglacial stress. *Quat. Sci. Rev.,* **22**(14), 1415-1426.

Clark, J.S. 1988. Stratigraphic charcoal analysis on petrographic thin sections: application to fire history in northwestern Minnesota. *Quat. Res.,* **30**(1), 81-91.

Clark, P.U. 1991. Striated clast pavements: products of deforming subglacial sediment? *Geology,* **19**(5), 530-533.

Clark, P.U. 1994. Unstable behavior of the Laurentide ice sheet over deforming sediment and its implications for climate change. *Quat. Res.,* **41**(1), 19-25.

Clark, P.U. 1997. Sediment deformation beneath the Laurentide Ice Sheet. *In* Martini, I.P., *ed. Late glacial and postglacial environmental changes, Quaternary, Carboniferous-Permian and Proterozoic.* Oxford University Press, New York, 81-97.

Clark, P.U. and J.S. Walder. 1994. Subglacial drainage, eskers, and deforming beds beneath the Laurentide and Eurasian ice sheets. *Geol. Soc. Am. Bull.,* **106**(2), 304-314.

Clark, P.U., R.B. Alley and D. Pollard. 1999. Northern hemisphere ice-sheet influences on global climate change. *Science,* **286**(5442), 1104 - 1111.

Clark, P.U., S.J. Marshall, G.K.C. Clarke, S.W. Hostetler, J.M. Licciardi, and J.T. Teller. 2001. Freshwater forcing of abrupt climate change during the last glaciation. *Science,* **293**(5528), 283-287.

Clayton, L. 1984. *Pleistocene geology of the Superior region, Wisconsin.* Wisconsin Geology Natural History Survey, Madison, WI, 1-40. (Information Cir. 46.)

Dowdeswell J.A.nand M.J. Sharp. 1986. Characterization of pebble fabrics in modern terrestrial glacigenic sediments. *Sedimentology,* **33**(5), 699-710.

Dowdeswell, J.A., M.J. Hambrey and R. Wu. 1985. A comparison of clast fabric and shape in Late Precambrian and modern glacigenic sediments. *J. Sediment. Petrol.,* **55**(5), 691-704.

Drake, L.D. 1977. Human factor in till fabric analysis. *Geology* **5**(3), 180-184.

Ensminger, S.L., E.B. Evenson, R.B. Alley, G.J. Larson, D.E. Lawson and J.C. Strasser. 1999. Example of the dependece of ice motion on subglacial drainge system evolution. *In* Mickelson, D.M. and J.W. Attig, eds. *Glacial processes Past and Present.* Geological Society of America, Boulder, Colorado, 11-21. (Special Paper 337.)

Evenson, E.B. 1971. The relationship of macro- and microfabric of till and the genesis of glacial landforms in Jefferson County, Wisconsin. In Goldthwait, R.P., ed. *Till, a symposium.* Ohio State University Press, Columbus, Ohio, 345-364.

Eyles, N., T.E. Day and A. Gavican. 1987. Depositional controls on the magnetic characteristics of lodgement tills and other glacial diamict facies. *Can. J. Earth Sci.,* **24**(12), 2436-2458.

Fischer, U.H. and G.K.C. Clarke. 2001. Review of subglacial hydro-mechanical coupling: Trapridge Glacier, Yukon Territory, *Canada. Quatern. Int.,* **86**(1), 29-43.

Freeze, R.A. and J.A. Cherry. 1979. Groundwater. Englewood Cliffs, Prentice-Hall, NJ.

Fuller, M.D. 1964. A magnetic fabric in till. *Geol. Mag*., **99**(3), 23-24.

Glen, J.W., J.J. Donner and R.G. West. 1957. On the mechanism by which stones in till become oriented. *Am. J. Sci.,* **255**(3), 194-205.

Gravenor, C.P. and M. Stupavsky. 1975. Convention for reporting magnetic anisotropy of till. *Can. J. Earth Sci.,* **12**(6), 1063-1069.

Gravenor, C.P., M. Stupavsky and D.T.A. Symons. 1973. Paleomagnetisim and its relationship to till deposition. *Can. J. Earth Sci.,* **10**(7), 1068-1078.

Ham, N.R. and D.M. Mickelson. 1994. Basal till fabric and deposition at Burroughs Glacier, Glacier Bay, Alaska. *Geol. Soc. Am. Bull.,* **106**(12), 1552-1559.

Hamilton, N. and A.I. Rees. 1970. The use of magnetic fabric in palaeocurrent estimation. *In* Runcorn S.K., *ed. Palaeogepphysics.* Academic Press, London and New York, 445-464.

Hart, J.K. 1994. Till fabric associated with deformable beds. *Earth Surf. Proc. Land.,* **19**(1), 15-32.

Hart, J.K. 1995. Subglacial erosion, deposition and deformation associated with deformable beds. *Prog. Phys. Geog.,* **19**(2), 173–191.

Hart, J.K. 1997. The relationship between drumlins and other forms of subglacial glaciotectonic deformation. *Quat. Sci. Rev.,***16**(1), 93-107.

Hart, J.K. and D.H. Roberts. 1994. Criteria to distinguish between subglacial glaciotectonic and glaciomarine sedimentation. I. Deformation styles and sedimentology. *Sediment. Geol.,* 91(1-4), 191-213.

Hart, J.K., F. Gane and R.J. Watts. 1996. Deforming bed conditions on the Dänischer Wohld Peninsula, northern Germany. *Boreas,* **25**, 101-113.

Hayman, N.W., B.A. Housen, T.T. Cladouhos and K. Levi. 2004. Magnetic and clast fabrics as measurements of grain-scale processes within the Death Valley shallow crustal detachment faults. *J. Geophys. Res.,* **109**(B05409), 1-16.

Hicock, S.R. 1992. Lobal interactions and rheologic superposition in subglacial till near Bradtville, Ontario, Canada. *Boreas,* **21**, 73-88.

Hicock, S.R. and A. Dreimanis. 1992. Deformation till in the Great Lakes regions: implications for rapid flow along the south-central margin of the Laurentide Ice Sheet. *Can. J. Earth Sci.,* **29**(7), 1565-1579.

Hicock, S.R., J.R. Goff, O.B. Lian and E.C. Little. 1996. On the interpretation of subglacial till fabric. *J. Sediment. Res.,* **66**(5), 928-934.

Hoffmann, K. and J.A. Piotrowski. Till mélange at Amsdorf, central Germany: sediment erosion, transport and deposition in a complex, soft-bedded subglacial system. *Sed. Geol.,* **140**(1-2), 215-234.

Hooyer, T.S. and N.R. Iverson. 2000. Clast-fabric development in a shearing granular material: implications for subglacial till and fault gouge. *Geol. Soc. Am. Bull.,* **112**(5), 683-692.

Hooyer, T.S., N.R. Iverson, F. Lagroix and J.F. Thomason. in press. Magnetic fabric of sheared till: a strain indicator for evaluating the bed-deformation model of glacier flow. J. *Geophys. Res.—Earth Surface.*

Howat, I.M., I. Joughin, S. Tulaczyk and S. Gogineni. 2005. Rapid retreat and acceleration of Helheim Glacier, east Greenland. *Geophys. Res. Lett.,* **32**, L22502, doi: 10.1029/2005GL024737.

Iken, A. and R.A. Bindschadler. 1986. Combined measurements of subglacial water pressure and surface velocity of the Findelengletscher, Switzerland: Conclusions about drainage system and sliding mechanism. *J. Glaciol.,* **43**(110), 101-119.

Iverson, N.R. 1999. Coupling between a glacier and a soft bed: II. model results. *J. Glaciol.,* **45**(149), 41-53.

Iverson, N.R., B. Hanson, R.LeB. Hooke and P Jansson. 1995. Flow mechanism of glaciers on soft beds. *Science,* **267**(5194), 80-81.

Iverson, N.R., D. Cohen, T.S. Hooyer, U.H. Fischer, M. Jackson, P.L. Moore, G. Lappegard and J. Kohler. 2003. Effects of basal debris on glacier flow. *Science,* **301**(5629), 81-84.

Iverson, N.R., R.W. Baker, R.LeB. Hooke, B. Hanson and P. Jansson. 1999. Coupling between a glacier and a soft bed: I. a relation between effective pressure and local shear stress determined from till elasticity. *J. Glaciol.,* **45**(149), 31-40.

Iverson, N.R., T.S. Hooyer and R.W. Baker. 1998. Ring-shear studies of till deformation: Coulomb-plastic behavior and distributed strain in glacier beds. *J. Glaciol.,* **44**(148), 634-642.

Iverson, N.R., T.S. Hooyer, J.F. Thomason, M. Graesch and J.R. Shumway. in press. The experimental basis for interpreting particle and magnetic fabrics of sheared till. *Earth Surf. Proc. Land.*

Iverson, N.R., T.S. Hooyer, U.H. Fischer, D. Cohen, P.L Moore, M. Jackson, G. Lappegard and J. Kohler. 2007. Soft-bed experiments beneath Engabreen, Norway: regelation infiltration, basal slip and bed deformation. *J. Glaciol.,* **53**(182), 323-340.

Jeffery, G.B. 1922. The motion of ellipsoidal particles immersed in a viscous fluid. *Proc. R. Soc. of Lon., Ser. A,* **102**, 169-179.

Jenson, J.W., P.U. Clark, D.R. MacAyeal, C. Ho and J.C. Vela. 1995. Numerical modeling of advective transport of saturated deforming sediment beneath the Lake Michigan lobe, Laurentide Ice Sheet. *Geomorphology,* **14**(2), 157-166.

Johnson, M.D. 1980. *Origin of the Lake Superior red clay and glacial history of Wisconsin's Lake Superior shoreline west of Bayfield Peninsula.* (unpublished M.S. thesis, University of Wisconsin.)

Johnson, M.D. 1983. The origin and microfabric of Lake Superior red clay. *J. Sediment. Petrol.,* **53**(3), 859-873.

Johnson, W.H. and A.K. Hansel. 1999. Wisconsinan episode glacial landscape of central Illinois: a product of subglacial deformation processes? *In* Mickelson, D.M. and J.W. Attig, *eds. Glacial processes Past and Present.* Geological Society of America, Boulder, Colorado, 121-135. (Special Paper 337.)

Kissel, C., C. Laj, A. Mazaud and T. Dokken. 1998. Magnetic anisotropy and environmental changes in two sedimentary cores from the Norwegian Sea and the North Atlantic. *Earth Planet. Sci. Lett.,* **164**(3-4), 617-626.

Klein, E.C. and D.M. Davis. 2002. Surface sample bias and clast fabric interpretation based on till, Ditch Plains, Long Island. *In* Hanson, G.N., *ed. Geology of Long Island and Metropolitan New York.* Long Island Geologists, State University of New York, 54-63.

Knight, J. 2002. Glacial sedimentary evidence supporting stick-slip basal ice flow. *Quat. Sci. Rev.,* **21**(8-9), 975-983.

Lappegard, G., J. Kohler, M. Jackson and J.O. Hagen. 2006. Characteristics of subglacial drainage systems deduced from load-cell measurements. *J. Glaciol.,* **52**(176), 137-148.

Larsen, N.K. and J.A. Piotrowski. 2003. Fabric pattern in a basal till succession and its significance for reconstructing subglacial processes. *J. Sediment Res.,* **73**(5), 725-734.

Larsen, N.K., J.A. Piotrowski and C. Kronborg. 2004. A mulitproxy study of a basal till: a time-transgressive accretion and deformation hypothesis. *J. Quat. Sci.,* **19**(1), 9-21.

Larsen, N.K., J.A. Piotrowski and F. Christiansen. 2006. Microstructures and microshears as proxy for strain in subglacial diamicts: implications for basal till formation. *Geology,* **34**(10), 889–892.

Larsen, N.K., J.A. Piotrowski and J. Menzies. in press. Microstructural evidence of low-strain, time-transgressive subglacial deformation. *J. Quat. Sci.,* DOI: 10.1002/jqs.1085.

Lawson, D.E. 1979. A comparison of the pebble orientation in ice and deposits of the Matanuska Glacier, Alaska. *J. Geol.,* **87**, 629-645.

Lian, O.B., S.R. Hicock and A. Dreimanis. 2003. Laurentide and Cordilleran fast ice flow: some sedimentological evidence from Wisconsinan subglacial till and its substrate. *Boreas,* **32**(1), 102–113.

Logan, J.M., C.A. Dengo, N.G. Higgs and Z.Z. Wang. 1992. Fabrics of experimental fault zones: their development and relationship to mechanical behavior. *In* Evans, G. and R.F. Wong, eds., *Fault Mechanics and Transport Properties of Rocks.* Academic Press, London, 33-67.

MacClintock, P. and A. Dreimanis. 1964. Reorientation of till fabric by overriding glacier in the St. Lawrence Valley. Am. *J. Sci.,* **262**(1), 133-142.

Mark, D.M. 1973. Analysis of axial orientation data, including till fabrics. *Geol. Soc. Am. Bull.,* **84**(4), 1369-1374.

Martin-Hernandez, F., C.M. Lüneburg, C. Aubourg and M. Jackson. 2004. Magnetic fabrics: methods and applications - an introduction. *In* Martin-Hernandez, F., C.M. Luneburg, C. Aubourg, M. Jackson, *eds., Magnetic fabric: methods and applications.* Geological Society, London, 1-7. (Special Publications 238.)

Menzies, J. 2000. Micromorphological analyses of microfabrics and microstructures indicative of deformation processes in glacial sediments. *In* Maltman, A.J., B. Hubbard, M.J. Hambrey, *eds., Deformation of Glacial Materials.* Geological Society, London, 245-257. (Special Publication 176.)

Menzies, J., J.J.M. van der Meer and J. Rose. 2006. Till—as a glacial "tectomict", its internal architecture, and the development of a "typing" method for till differentiation. *Geomorphology,* **75**(1-2), 172-200.

Morgenstern, N.R. and J.S. Tchalenko. 1967. Microscopic structures in kaolin subjected to direct shear. *Géotechnique,* **17**, 309-328.

Moss, C.M. 1977. *The surficial and environmental geology of the French River quadrangle St. Louis County, Minnesota. (unpublished M.S. thesis, University of Minnesota, Duluth.)*

Murray, T and G.K.C. Clarke. 1995. Black-box modelling of the subglacial water system. *J. Geophys. Res.*, **86**, 29-43.

Need, E.A. 1980. *Till stratigraphy of Wisconsin's Lake Superior shoreline: Wisconsin Point to Bark River: Part I.* (unpublished M.S. thesis, University of Wisconsin.)

Need, E.A. and M.D. Johnson. 1980. *Glacial history of Wisconsin's Lake Superior shoreline: Wisconsin Point to Bark River, in Origin of the Lake Superior red clay and glacial history of Wisconsin's Lake Superior shoreline west of Bayfield Peninsula.* (unpublished M.S. thesis, University of Wisconsin.)

Nowaczyk, N.R. 2003. Detailed study on the anisotropy of magnetic susceptibility of arctic marine sediments. *Geophys. J. Int.,* **152**(2), 302-317.

Park, C.K, S.J. Doh, D.W. Suk and K.H. Kim. 2000. Sedimentary fabric on deep-sea sediments from KODOS area in the eastern Pacific. *Mar. Geol.,* **171**(1-4), 115-126.

Piotrowski, J.A. and A.M. Kraus. 1997. Response of sediment to ice-sheet loading in northwestern Germany: effective stresses and glacier-bed stability. *J. Glaciol.,* **43**(145), 495-502.

Piotrowski, J.A., D.M. Mickelson, S. Tulaczyk, D. Krzyszkowski and F.W. Junge. 2001. Were deforming subglacial beds beneath past ice sheets really widespread? *Quatern. Int.,* **86**(1), 139-150.

Piotrowski, J.A., D.M. Mickelson, S. Tulaczyk, D. Krzyszkowski and F.W. Junge. 2002. Reply to the comments by G.S. Boulton, K.E. Dobbie, S. Zatsepin on: deforming soft beds under ice seets: how extensive were they? *Quatern. Int.,* **97-98**, 173-177.

Piotrowski, J.A., N.K. Larsen and F.W. Junge. 2004. Reflections on soft subglacial beds as a mosaic of deforming and stable spots. *Quat. Sci. Rev.,* **23**(9-10), 993-1000.

Piotrowski, J.A., N.K. Larsen, J. Menzies and W. Wysota. 2006. Formation of subglacial till under transient bed conditions: deposition, deformation, and basal decoupling under a Weichselian ice sheet lobe, central Poland. *Sedimentology,* **53**(1), 83-106.

Piotrowski, J.A., U. Döring, A. Harder, R. Qadirie and S. Wenghöfer. 1997. 'Deforming bed conditions on the Danischer Wohld Peninsula, northern Germany': comments. *Boreas,* **26**, 73-33.

Principato, S.M., A.E. Jennings, G.B. Kristjánsdóttir and J.T. Andrews. 2005. Glacial-marine or subglacial origin of diamicton units from the Southwest and North Iceland Shelf: implications for the glacial history of Iceland. *J. Sediment Res.,* **75**(6), 968–983. DOI: 10.2110/jsr.2005.073

Rignot, E. and R. Kanagaratnam. 2006. Changes in the velocity structure of the Greenland Ice Sheet. *Science,* **211**(5763), 986-990.

Simpkins, W.W., S.A. Rodenbeck and D.M. Mickelson. 1990. Geotechnical and hydrological properties of till stratigraphic units in Wisconsin. *In* Lagerlund, E., ed., *Methods and Problems of Till-Stratigraphy.*, 11-15. (LUNDQUA Report, vol. 32.)

Skempton, A.W. 1985. Residual strength of clays in landslides, folded strata and the laboratory. *Géotechnique,* **35**(1), 3-18.

Stephenson, D.A., A.H. Fleming and D.M. Mickelson. 1988. Glacial deposits. *In* Back, W., J.S. Rosenshein and P.R. Seaber, *eds., Hydrogeology.* Geological Society of America, Boulder Colorado. (The Geology of North America, v.O-2.)

Stewart, R.A., D. Bryant and M.J. Sweat. 1988. Nature and origin of corrugated ground moraine of the Des Moines Lobe, Story County, Iowa. *Geomorphology,* **1**(2), 111-130.

Stuiver, M. and 9 others. 1998. INTERCAL98 radiocarbon age calibration, 24,000 - 0 cal BP. *Radiocarbon,* **40**(3), 1041-1083.

Stupavsky, M. and C.P. Gravenor. 1975. Magnetic fabric around boulders in till. Geol. *Soc. Am. Bull.,* **86**(11), 1534-1536.

Stupavsky, M., C.P. Gravenor and D.T.A. Symons. 1974. Paleomagnetism and magnetic fabric of the Leaside and Sunnybrook Tills near Toronto, Ontario. *Geol. Soc. Am. Bull.,* **85**(8), 1233-1236.

Tarling, D.H. and F. Hrouda. 1993. *The Magnetic Anisotropy of Rocks.* Chapman and Hall, London.

Thomason, J.F. and N.R. Iverson. 2006. Microfabric and microshear evolution in deformed till. *Quat. Sci. Rev.,* **25**(9-10), 1027-1038.

Thomason, J.F.. 2006. *In Laboratory studies of till deformation with implications for the motion and sediment transport of the Lake Michigan lobe.* (Ph.D. dissertation, Iowa State University.)

Truffer, M. and W.D. Harrison. 2006. In situ measurements of till deformation and water pressure. *J. Glaciol.,* **52**(177), 175-182.

Truffer, M., W.D. Harrison and K.A. Echelmeyer. 2000. Glacier motion dominated by processes deep in underlying till. *J. Glaciol.,* **46**(153), 213-221.

Tulaczyk, S., W.B. Kamb and H.F. Engelhardt. 2000. Basal mechanics of Ice Stream B, West Antarctica 1. till mechanics. *J. Geophys. Res.* **105**(B1), 463-481.

van der Meer, J.J.M. 1993. Microscopic evidence of subglacial deformation. *Quat. Sci. Rev.,* **12**(7), 553-587.

van der Meer, J.J.M., J. Menzies and J. Rose. 2003. Subglacial till: the deforming glacier *bed. Quat. Sci. Rev.,* 22(15-17), 1659-1685.

van der Wateren, F.M., S.J. Kluiving and L.R. Bartek. 2000. Kinematic indicators of subglacial shearing. *In* Maltman, A.J., B. Hubbard and M.J. Hambrey, *eds., Deformation of Glacial Materials.* Geological Society, London, 259-278. (Special Publication 176.)

Wright, H.E., C.L. Matsch and E.J. Cushing. 1973. Superior and Des Moines Lobes. *In* Black, R.F., R.P. Goldthwait and H.B. Willman, *eds. The Wisconsinan Stage.* Geological Society of America, Boulder Colorado, 153-185. (Geol. Soc. Am. Mem. 136.)

Yi Chaolu and Cui Zhijiu. 2001. Subglacial deformation: evidence from microfabric studies of particles and voids in till from the upper Ürümqui river valley, Tien Shan, China. *J. Glaciol.,* **47**(159), 607-612.

Zarth, R.J. 1977. *The Quaternary geology of the Wrenshall and Frogner quadrangles, northeastern, Minnesota.* (unpublished M.S. thesis, University of Minnesota, Duluth.)